

Pollution Without Borders: Transboundary Air Pollution and the Geography of Pollutant Control Policy *

Yuanhang Yu [†]

London School of Economics

Antonio Avila-Uribe [‡]

Joint Research Centre, European Commission

February 10, 2026

Click here for the latest version

Abstract

Air pollution disperses across political boundaries, yet many environmental policies regulate specific polluted locations. This paper studies how cross-boundary transport of fine particulate matter ($PM_{2.5}$) changes the welfare effect and optimal design of pollutant control policy in China. Using particle trajectory data from atmospheric transport models, we construct bilateral pollutant-flow matrices that measure the transboundary air pollution in China. Three patterns emerge: (1) Transboundary pollution contributes heterogeneously to local $PM_{2.5}$, accounting for less than 10% to over 50% of provincial concentrations; (2) Bilateral pollutant transport networks remain stable over time, enabling long-term policy coordination without frequent recalibration; and (3) Economically developed provinces in China receive more transboundary pollution yet achieve larger pollution reduction. We develop a dynamic spatial general equilibrium model that incorporates pollutant transport, trade, and migration. Using this model, we estimate that transboundary air pollution creates a 1% national welfare loss relative to a counterfactual where pollution remains local. We evaluate China's Air Pollution Prevention and Control Action Plan and compare it to alternative allocation rules. Reallocating abatement target to high-spillover upwind provinces based on marginal social welfare of emission tax improves aggregate welfare by 0.18% relative to the actual policy. The findings reveal welfare gains from accounting for spatial externalities in policy design.

*We thank Thomas Sampson, Daniel Sturm, Clare Balboni, Jose Vasquez, Catherine Thomas who provide valuable supports and feedback to the project. For insightful advice, we thank Esteban Rossi-Hansberg, Adrien Bilal, Michael Peters, Joseph Shapiro, Ahmad Lashkaripour, Robin Burgess, Gharad Bryan, David Baqaee, Teresa Fort, Chenzi Xu, Wei Xiang, Allan Hsiao, Animesh Jayant, Emiliano Rinaldi, Stephan Thies, and numerous seminar and conference participants, especially at LSE international seminar, LSE trade and urban seminar, LSE EEE seminar, UEA North America, ICCDS (SJTU Antai), and CUHK summer school of Asia in the global economy.

[†]Department of Economics, London School of Economics. Email: y.yu42@lse.ac.uk

[‡]Department of Geography and Environment, London School of Economics. Email: a.avila2@lse.ac.uk

1 Introduction

A central challenge in environmental regulation arises when pollution damages extend far beyond its origin. In decentralized systems, jurisdictions set abatement targets by weighing local benefits and costs, often neglecting the external harms imposed on downwind or downstream neighbors. Centralized governments face parallel challenges in designing efficient and equitable pollutant control policy when pollution crosses internal administrative boundaries. This divergence between private incentives and social cost creates a misalignment in regulatory effort. The question of how to design institutions that internalize such cross-boundary externalities has engaged economists since the seminal work of [Pigou \(1920\)](#) and [Coase \(1960\)](#), yet remains central to modern environmental policy debates from acid rain treaties ([CLRTAP, 1979](#)) to carbon border adjustments ([Ambec, Esposito and Pacelli, 2024](#)).

Transboundary air pollution is an important example of this problem. Globally, air pollution accounts for more than 4 million premature deaths each year worldwide ([GBD, 2020](#); [HEI, 2022](#)), and fine particulate matter (PM_{2.5}) exposure alone shortens global life expectancy by about 2.2 years ([Greenstone, Hasenkopf and Lee, 2022](#)). Prevailing winds can carry PM_{2.5} hundreds of kilometers across provincial and national borders ([Lin et al., 2014](#)), so damages also occur in places far from the source. In East Asia, pollution originating in China increases mortality and morbidity in South Korea ([Heo, Ito and Kotamarthi, 2023](#)); In North America, long-range wildfire smoke has been shown to reduce local earnings and labour force participation ([Borgschulte, Molitor and Zou, 2024](#)). These facts underscore that transboundary pollution can disrupt economic activity far from its source, thereby creating a rationale for regulations that account for such spatial externalities.

This paper quantifies the welfare impact of transboundary PM_{2.5} in China and studies its implications for pollutant control policies. We combine physically calibrated pollutant-flow matrices, estimated from particle trajectory data, with a dynamic quantitative spatial general equilibrium model that connects households, firms, and the atmosphere. This framework maps upwind emissions into downwind pollution exposure and economic outcomes, enabling us to measure the welfare cost of pollutant dispersion and to compare China's Air Pollution Prevention and Control Action Plan (APPCAP) with counterfactual allocation rules.

We proceed in two steps. First, we construct province-to-province pollutant-flow matrices using particle trajectory data from the Hybrid Single-Particle Lagrangian Integrated Trajectory (HYSPLIT) model. These matrices quantify the magnitude and direction of cross-provincial PM_{2.5} dispersion, capturing how pollution in one province is carried by wind to contribute to ambient pollution in others. Second, we integrate these transport matrices into a dynamic spatial equilibrium model in which migration choices, production, and pollution dispersion are jointly determined. Following [Caliendo, Dvorkin and Parro \(2019\)](#), households are forward-looking and choose where to live and work, trading off local consumption and amenities. Migration is frictionless across sectors, costly across provinces. Firms hire labour and purchase intermediate inputs to produce output, emitting PM_{2.5} as a byproduct subject to taxation ([Caliendo and Parro, 2015](#); [Taylor and](#)

[Copeland, 2003](#)). Crucially, pollutant particles are not confined to their origin: the atmosphere reallocates PM_{2.5} across provinces according to the flow matrices which determines local pollution levels. Ambient PM_{2.5} affects economic outcomes through two channels: higher PM_{2.5} reduces local productivity ([Fu, Viard and Zhang, 2021](#)) and lowers amenity values ([Deryugina et al., 2019](#)). These feedback effects trigger adjustments in wages, rents, and migration, reshaping the spatial distribution of economic activities. Relative to recent advances in quantitative spatial models, our key contribution is integrating an atmospheric block with physically-calibrated pollution transport, allowing the geography of air flows to shape the geography of welfare and policy incidence. With the calibrated model, we quantify the welfare effect from pollutant dispersion and compare APPCAP to other allocation rules.

Recent advances in atmospheric modeling provide new data sources that enable researchers to trace pollution transport with more precision. Atmospheric scientists have developed direct measurements of particle trajectories using models like HYSPLIT, which simulate how individual air masses move through the atmosphere based on wind patterns, temperature gradients, and topography. We combine HYSPLIT trajectory data with econometric methods to estimate pollution passthrough rates—the marginal contribution of upwind pollution to downwind regions. Using these estimates, we construct bilateral pollutant-flow matrices that quantify the share of each province's PM_{2.5} attributable to pollution from every other province. Our estimated flow matrices reveal three key patterns in China. First, spatial heterogeneity in transboundary exposure is substantial. Inland provinces like Xinjiang receive minimal transboundary air pollution, implying that majority of their ambient PM_{2.5} originates locally. In contrast, coastal manufacturing provinces experience heavy transboundary burdens: in 2017, Shanghai and Jiangsu receive 50 – 60% of their ambient PM_{2.5} from upwind provinces, with Beijing and Tianjin similarly exposed at 40 – 50%. This geographic pattern reflects prevailing wind corridors: winds transport pollution from inland regions in the north and west toward the densely populated North China Plain and Yangtze River Delta. Second, the upwind-downwind network remains stable over time. The core structure of upwind-downwind linkages persists across years despite short-term meteorological variation. Correlation between flow matrices estimated for different five-year periods exceeds 0.9, indicating that atmospheric geography not transient weather governs dispersion. This temporal stability implies that policies targeting transboundary transport remain effective over the long term without frequent recalibration. Third, transboundary exposure correlates strongly with economic development. Provinces with higher GDP per capita systematically receive larger pollution inflows. Shanghai, Jiangsu, and Zhejiang, among China's wealthiest provinces, face substantial transboundary shares, ranging from 45% to 55%. Yet these same regions achieved greater percentage reduction in PM_{2.5} concentration during China's 2013-2018 APPCAP campaign. This pattern where regions receive substantial pollution inflows yet also undertake larger pollution reductions raises a key question: who ultimately bore the cost of cleaning up China's air?

In the second step, we construct a spatial general equilibrium model with both physical and

economic geography. We calibrate the model to 30 Chinese provinces and municipalities, parameterizing three key sets of parameters that are critical for quantifying the welfare effects of pollution and corresponding policy responses. First, emission elasticities capture the responsiveness of emission with respect to abatement. We infer them from observed variation in emission productivity, defined as output per unit of emission, across sectors, assuming technological differences rather than tax variation drive the cross-sectoral patterns. Second, the externality coefficients quantify the negative impact of pollution on local productivity and amenities. Estimating these parameters faces an endogeneity problem: local pollution is correlated with unobserved local characteristics. To address endogeneity, we employ thermal inversions—meteorological phenomena that mechanically trap pollutants near the surface—as an instrumental variable for local air quality, following the established practice in the reduced-form literature. Third, the deposition rate governs how quickly airborne PM_{2.5} settles or is removed from the atmosphere, determining the persistence of trans-boundary externalities. We estimate it by fitting the model’s predicted concentration evolution to observed satellite data across time. We also invert productivity, amenity and emission from the model. Productivity is recovered by matching the sectoral value-added. Amenity values are inferred from observed migration flow data using the migration share equations. The emission tax in the baseline economy is inverted from the firm’s first-order condition, which represents the shadow price of emissions and reflects the stringency of local environmental regulation.

We use the calibrated model to conduct counterfactual exercises that isolate the welfare consequences of transboundary pollution and evaluate pollutant control policies. The first exercise quantifies the welfare cost of atmospheric dispersion by comparing the calibrated spatial equilibrium to a counterfactual where pollution remains fully local. Our results indicate that transboundary air pollution decreases national welfare by 1% in consumption-equivalent terms relative to a scenario without cross-regional dispersion. This aggregate gain masks sharp geographic redistribution. Upwind provinces in the north and northwest would experience a welfare decline of over 4% if atmospheric dispersion were not allowed, as they would no longer be able to export pollution to downwind regions. In contrast, eastern and southeastern manufacturing provinces—such as Jiangsu, Shanxi, and Shandong, which currently receive substantial transboundary inflows—would see welfare gains of around 6% if all pollution were only retained locally. To isolate the mechanisms through which transboundary pollution affects welfare, we decompose the aggregate cost by sequentially disabling migration responses and pollution externality on amenity and productivity. We find that amenity effects dominate: shutting down the negative effect on amenity reduces the welfare cost of transboundary transport from 1% to 0.45%, indicating that direct quality-of-life impacts account for approximately 55% of the total loss. Productivity effects contribute roughly one-third of the welfare cost. Migration plays a limited role, contributing around 0.1 percentage points.

A second set of exercises evaluates China’s APPCAP and compares it to alternative allocation rules. In 2013, China’s State Council launched the Air Pollution Prevention and Control Action Plan. The policy mandated differentiated PM_{2.5} reduction targets for three key economic regions,

requiring that their PM_{2.5} concentration levels by 2017 fall by 25% in the Beijing-Tianjin-Hebei region, 20% in the Yangtze River Delta, and 15% in the Pearl River Delta, relative to 2013 levels. This policy concentrated regulatory effort in regions with severe local pollution and high political visibility. While APPCAP differentiates targets spatially, neither the policy design nor official documentation indicates explicit consideration of transboundary pollution flows. To evaluate the welfare effects of APPCAP, we simulate its introduction in a dynamic spatial equilibrium model from a 2012 baseline. We first reconstruct the province-specific emission reduction targets set for 2017 under the policy, and then infer the shadow tax rates required to achieve them. Our results show that the APPCAP increased national welfare by 0.2% relative to a counterfactual scenario in which shadow emission tax rates after 2012 remained fixed at their 2012 levels.

We compare the APPCAP to alternative allocation rules, holding fixed the aggregate emission reduction calculated by applying APPCAP’s regional targets to the 2012 baseline economy. We consider three policy scenarios with varying allocation principles. Uniform allocation assigns equal absolute cuts to all provinces, yielding higher percentage reductions for small emitters and lower reductions for large ones. Emission-share allocation assigns cuts proportional to baseline emissions, implementing a uniform reduction rate of approximately 0.6% across provinces. Marginal-welfare-weighted allocation assigns reduction responsibilities proportional to each province’s marginal social value of emission tax. This marginal social value is derived from the model by simulating a small emission tax increase in each province—holding all other provinces’ taxes constant—and measuring the resulting change in national welfare. This approach concentrates abatement where marginal social returns of emission tax are highest: upwind inland provinces whose emissions reach populous downwind regions receive large reduction responsibilities, while provinces with near-zero returns face minimal requirements.

The results reveal welfare gains from accounting for spatial externalities. Relative to APPCAP, uniform allocation performs worse, reducing national welfare by 0.12%. The emission-share allocation outperforms the APPCAP by a small margin, increasing national welfare by 0.02%. The marginal-welfare-weighted rule delivers the largest gains, improving aggregate welfare by 0.18%. This rule concentrates abatement in upwind inland provinces where emissions travel to densely populated downwind regions, generating outsized national benefits per unit of abatement. In contrast, coastal provinces like Guangdong and Jiangsu, whose emissions largely remain local, face minimal reduction requirements under the welfare-weighted rule. Our results highlight the welfare improvement of aligning environmental regulation with atmospheric transport patterns. This implies that regulatory efficiency depends not only on where pollution is emitted, but also on where it is deposited, arguing for policy instruments that internalize cross-jurisdictional spillovers.

Related literature and contributions — This paper contributes to three strands of literature. The first one is to study the economic impact of air pollution. Research in this field has established a causal link between local air pollution and various health outcomes, including infant and adult mortality ([Ebenstein et al., 2015](#); [Arceo, Hanna and Oliva, 2016](#); [Deryugina et al., 2019](#); [Heo, Ito](#)

and Kotamarthi, 2023). Studies on labor market outcomes have also documented negative effects on work hours, productivity, and income (Zivin and Neidell, 2012; Hanna and Oliva, 2015; Fu, Viard and Zhang, 2021; Borgschulte, Molitor and Zou, 2024). Chen, Oliva and Zhang (2022) provides the first causal estimate of the impact of air pollution on migration in China, thereby connecting air quality to the spatial distribution of economic activities. A few papers focus on the effect from the transboundary nature of air pollution (Heo, Ito and Kotamarthi, 2023; Borgschulte, Molitor and Zou, 2024; Fu, Viard and Zhang, 2022). Our paper extends this line of inquiry by moving beyond reduced-form estimates to develop a dynamic spatial general equilibrium framework. This approach allows us to integrate multiple adaptive mechanisms and jointly determine the welfare and distributional consequences of transboundary pollution through endogenous adjustments in prices, wages, and labour.

This paper also contributes to the literature that applies integrated assessment models (IAMs) to environmental and climate policy analysis. IAM is a multidisciplinary approach that unites perspectives from economics, environmental science, and energy systems to analyze complex issues that involve interactions between human and natural systems. IAMs have been used to study global warming, sea level rise, and the macroeconomic effects of rising temperatures (Balboni, 2025; Bilal and Käenzig, 2024; Cruz and Rossi-Hansberg, 2024). Existing integrated assessment models and spatial general equilibrium models typically abstract from transboundary air pollution and its economic effects (Khanna et al., 2021; Hebligh, Trew and Zylberberg, 2021). To address this gap, we develop a new model that combines particle dispersion channel with an economic geography framework, explicitly accounting for cross-regional pollutant transport. This allows us to quantify the welfare impacts of various policies while capturing the environmental and economic feedback loops of pollution spillovers.

Lastly, this paper contributes to the growing literature of spatial environmental economics, which examines how the spatial distribution of economic activity shapes environmental outcomes and how environmental goods, in turn, feed back into economic geography (Balboni and Shapiro, 2025; Domínguez-Iino, 2023). A central question in this field is how to design spatial environmental policy that explicitly account for the environmental spillovers. A first branch of this literature studies cap-and-trade with spatial differentiation. Building on Montgomery (1972), Fowlie and Muller (2013) show how trading ratios keyed to heterogeneous marginal damages can improve efficiency relative to uniform permits, and Chan et al. (2018) quantify the welfare and incidence consequences when markets ignore where emissions occur and where exposure happens. These papers clarify when and how trades should be weighted by location to align private incentives with social damages.

A second strand of literature examines non-market approaches to manage cross-jurisdictional environmental spillovers. These can be broadly grouped into two categories. The first is command-and-control regulation, which remains the dominant policy instrument in both the United States (e.g., the Clean Water Act and Clean Air Act) and China (e.g., target- and concentration-based controls). While command-and-control has proven effective in regulating well-identified point sources,

it performs poorly in managing non-point and cross-boundary pollution (Chen, Li and Lu, 2018). A second category of hybrid transfer mechanisms has been implemented in settings like river basins, where clear directional externalities enable governments to negotiate transfers. Evidence from China’s Xin’an River program confirms that such approaches can align local abatement with basin-wide goals (Chen et al., 2022; Wang, Xu and Chen, 2025). Nevertheless, command-and-control remains the dominant regulatory framework in major economies, and its efficacy in spatially complex environments remains an open question.

This paper makes three contributions to the literature on spatial environmental economics. First, we develop a spatial general equilibrium framework that integrates goods trade, labor mobility, and transboundary pollutant flows, providing a unified structure to analyze policy incidence under cross-jurisdictional externalities. Second, we provide the first quantitative evaluation of China’s command-and-control air pollution policies that explicitly accounts for atmospheric transport, bridging physical geography with economic geography. Third, we design and compare spatially differentiated regulatory rules that internalize pollution spillovers, and compare it to the China’s policy.

The paper is organized as follows. First, we introduce the data sources, with a particular focus on the trajectory data used in this study. Next, we present the stylized facts and empirical evidence, documenting the transboundary air pollution pattern in China. Then, we introduce the spatial model, outlining its structure and key assumptions. Finally, we discuss the model simulation results.

2 Data

We draw on diverse datasets from meteorological models, satellite images, and government surveys to inform our analysis. This section briefly describe each source.

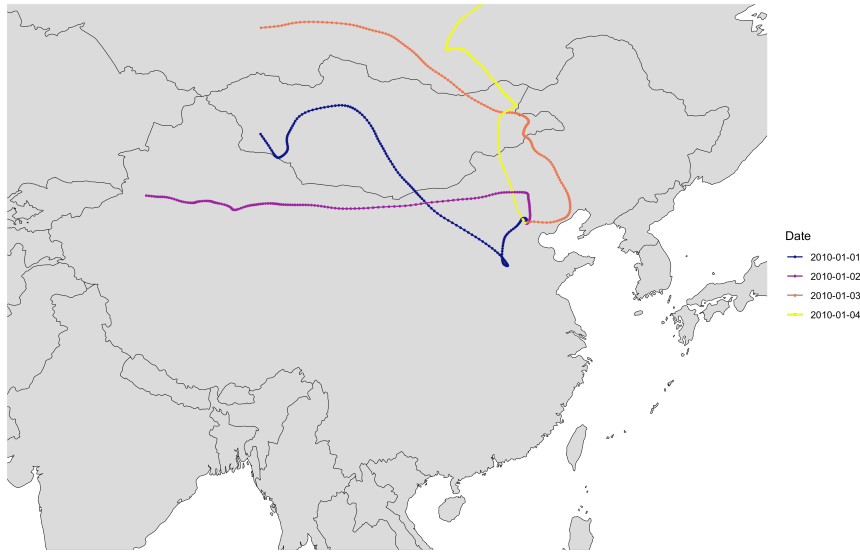
2.1 Particle Trajectory Data from HYSPLIT

Researchers in atmospheric science have developed meteorological model to obtain direct measures of particle trajectory. The model can compute trajectories of particles to determine how far and to where particles travel through. A trajectory is a time-stamped sequence of latitude-longitude-height points describing where an infinitesimal particle of air travels. In atmospheric science, back trajectories are extremely useful in air pollution analysis and can provide important information on air mass origins. One of the state-of-the art methods is the Hybrid Single-Particle Lagrangian Integrated Trajectory model (HYSPLIT), which has been developed by the National Oceanic and Atmospheric Administration (NOAA) Air Resources Laboratory. HYSPLIT has been used in a variety of applications to describe atmospheric transport, dispersion, and deposition of pollutants. By launching many such trajectories from specified locations and heights, researchers can characterize how far, how fast, and in which directions pollution plumes are transported, independent of local

policy or monitoring density.

We employ the HYSPLIT model to generate backward trajectories for each grid cell within China. We compile trajectory data for each day from 2002 to 2017. For each grid cell, we use the HYSPLIT model to trace backward trajectories spanning up to 168 hours, mapping the path of air masses arriving at each location. HYSPLIT provides the particle trajectory's data on its longitude, latitude and height every hour. Figure 1 shows the backward trajectory arriving in Beijing on different days in January 2010. As shown in the graph, there is one trajectory for each day, all generated at the same time within the day. Geolocation data are recorded hourly along the trajectory, extending up to 168 hours backward in time. For the majority of the time, the air mass arriving in Beijing originates from the north. However, there are still variations in terms of the areas the trajectory travels through. We also obtained the climatic conditions for each point along the trajectory. By integrating this information with pollution data, we can construct a comprehensive picture of the climate and pollution conditions for each grid cell as the air mass travels to these locations.

Figure 1: Backward Trajectory Arrives in Beijing



Notes: This figure displays the backward trajectories arriving in Beijing on different days in January 2010.

We use these trajectories to measure how much PM_{2.5} an air mass can pick up and carry from each upwind province to each downwind province. Concretely, for every receptor location and day we intersect the back-trajectory path with provincial borders and record where the air mass traveled, how long it lingered, and under what meteorological conditions. We combine this path information with gridded PM_{2.5} to estimate a passthrough relationship. Intuitively, air passing through more polluted areas carries a higher particulate load, which impacts air quality at the locations where the air mass deposits. Variation in wind direction provides the necessary variation to estimate pollutant passthrough.

2.2 PM_{2.5} data

We utilise PM_{2.5} concentration data from the Atmospheric Composition Analysis Group at Washington University in St. Louis ([Van Donkelaar et al., 2021](#)), which estimates PM_{2.5} concentration by combining Aerosol Optical Depth (AOD) retrievals from satellite with the GEOS-Chem chemical transport model and calibrating to ground-based observations based on a Geographically Weighted Regression (GWR). This dataset provides monthly ground-level PM_{2.5} concentrations with high spatial resolution from 1998 to 2018, allowing for the matching with trajectory data. PM_{2.5} emissions are from the Emission Database for Global Atmospheric Research (EDGAR) ([Crippa et al., 2020](#)). This database provides annual emissions data for greenhouse gases and local air pollutants, including PM_{2.5}, per sector and country for 1970-2022. EDGAR calculates emissions based on the emission factor approach, using the detailed information on the emission factor of each activity and different emission-reducing technology installation.¹ EDGAR provides both emissions as national totals and gridmaps at 0.1 × 0.1 degree resolution at global level.

2.3 Weather data

We use the MERRA-2, the Modern-Era Retrospective analysis for Research and Applications. This is an advanced atmospheric reanalysis dataset produced by NASA's Global Modeling and Assimilation Office (GMAO). MERRA-2 provides comprehensive global climate data spanning from 1980 to the present, incorporating a vast array of observations from satellite, aircraft, and surface-based measurement systems. The dataset includes numerous atmospheric parameters, such as temperature, humidity, wind, and surface pressure, along with surface fluxes and land surface variables. This extensive dataset enables a detailed characterization of the climatic conditions at gridded locations.

2.4 Provincial economic data

We obtain economic variables such as GDP and population for Chinese province from China Statistical Yearbook. We use the Chinese Input-Output table compiled by the National Bureau of Statistics of China to obtain regional trade flows. Specifically, we utilize the version processed by [Zhao et al. \(2024\)](#), which addresses discrepancies across the original yearly data and produces a continuous, consistent dataset. We use the data for the years 2002, 2007, 2012 and 2017. We also obtain provincial migration data from the Census. Given the data limitation, we obtain migration data for years 2000, 2005 and 2010.

¹In other words, the database is not direct observations of emissions. See the dataset's web page (<https://edgar.jrc.ec.europa.eu/>) for more details.

3 Geographic Pattern of Transboundary Air Pollution in China

This section characterizes transboundary air pollution in China. Specifically, we want to understand how pollution in one province travels and affect populations elsewhere. Using particle trajectory data, we first estimate pollutant passthrough rates that describe how PM_{2.5} disperses across space. Using these estimates, we construct a bilateral pollutant-flow matrix, where it measures the share of PM_{2.5} in receptor province attributable to pollution from other provinces. These matrices provide a quantitative description of cross-regional pollutant dispersion. Three stylized facts emerge from these matrices :

- **Pattern I: Heterogeneous inflow contributions.** The share of PM_{2.5} coming from other provinces varies markedly across space; some provinces are dominated by local sources, while others heavily affected by upwind inflows.
- **Pattern II: Limited temporal change.** Across years, the bilateral transport network is rather stable. While we observe minor fluctuations and noise, the core structure of the transport network remains stable over time, indicating that underlying geographic features and prevailing wind patterns exhibit little change across the study period.
- **Pattern III: Developed downwind receptors.** Economically advanced coastal provinces in China receive more transboundary contributions from inland upwind regions. Northern and northwestern provinces are major sources affecting the country's main economic hubs along the coast.

These findings form the foundation for evaluating the welfare and policy implications of transboundary air pollution, which we explore further through a quantitative spatial general equilibrium model. In the following sections, we first detail our econometric approach to estimate the PM_{2.5} passthrough function and how we construct the bilateral flow matrices. We present and discuss three stylized facts derived from these matrices, providing empirical insights that motivate and inform the structural modelling analysis.

3.1 Estimating PM_{2.5} Passthrough Rates and the Bilateral pollutant-flow Matrix

To quantify transboundary air pollution in China, a crucial first step is to understand how PM_{2.5} dissipates across space. We adopt the concentric ring approach, a method inspired by urban economics and notably used to study the decay of knowledge spillovers within cities (Henderson, 2007), to estimate the pollution passthrough function. Intuitively, the concentric ring method divides the study area into a series of rings centered on a focal point. It examines how the intensity of spillovers changes as one moves outward through these rings. Each ring represents a distance band from the source, within which the concentration of pollutants is expected to decrease due to factors like dilution and dispersion. By applying this framework to air pollution, we systematically quantify how

$\text{PM}_{2.5}$ concentrations weaken as pollution travels away from emitting sources, capturing the geographic decay of airborne particulate matter. This provides a transparent and empirically grounded way to measure the spatial extent of transboundary pollution.

To model the relationship between local $\text{PM}_{2.5}$ and transported pollution, we estimate the following specification:

$$\text{DestPM}_{it} = \sum_{h=1}^{28} (\alpha_h + \beta_h \text{TrajPM}_{h,it} + \gamma_h \text{Weather}_{h,it}) + \delta_i + \delta_{my} + \epsilon_{it},$$

where DestPM_{it} denotes the $\text{PM}_{2.5}$ concentration at destination grid cell i at day t , TrajPM_{it} represents $\text{PM}_{2.5}$ concentration at a location along the trajectory that lands in location i . The variable Weather_{it} controls for a set of time-varying atmospheric conditions along the trajectory that influence $\text{PM}_{2.5}$ dispersion, including precipitation, wind speed, pressure, temperature, and humidity. We segment particle trajectories into six-hour travel time intervals, indexed by h . β_h is the key coefficient, measuring the marginal impact of $\text{PM}_{2.5}$ at locations h hours upwind on destination $\text{PM}_{2.5}$. The regression includes location fixed effects (δ_i) to control for time-invariant local characteristics and month-by-year fixed effects (δ_{my}) to account for common temporal factors that may affect pollution levels. We estimate the equations on a destination-day panel from 2002–2017. The destination unit i is a $25 \text{ km} \times 25 \text{ km}$ grid cell in China. For each grid cell on day t , we collect one 168-hour back-trajectory tracing back up to 7 days. This trajectory is divided into 28 segments of six hours each, indexed by $h \in \{1, \dots, 28\}$.

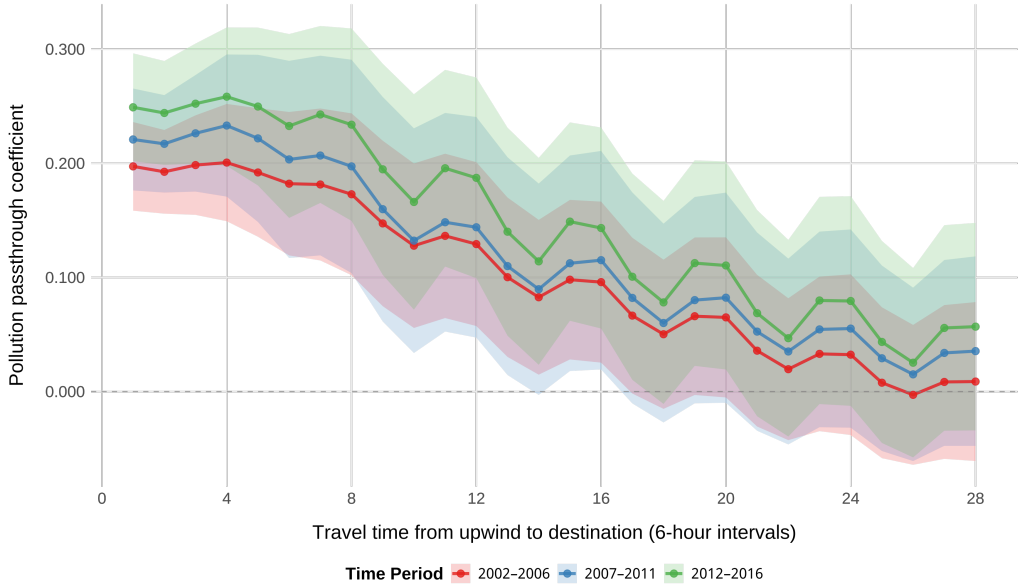
The identifying variation arises from changes in particle trajectories caused by randomness in atmospheric transport and fluctuations in wind direction. Within a given destination grid cell and month-year, the $\text{PM}_{2.5}$ concentration data is fixed with the monthly concentration data. However, daily fluctuations in wind direction alter the particle trajectories, causing the paths of air masses to vary from day to day. This randomness results in different routes being taken by the air mass, passing through distinct upwind regions before reaching a specific location. Since we apply the same monthly $\text{PM}_{2.5}$ map to all these varied trajectories, the day-to-day changes in TrajPM_{it} reflect differences in trajectory geometry rather than any within-month changes in upwind $\text{PM}_{2.5}$. The regression design with destination fixed effects and time fixed effects therefore compares days within the same destination and month–year environment that differ mainly in the mix of upwind origins and the residence time along the path. We allow the passthrough rates to vary flexibly with upwind travel time. The identifying assumption is that, after controlling for these factors, the specific upwind cells influencing a given destination on any day are plausibly quasi-random with respect to local economic activities. Therefore, the estimated β_h trace out a causal passthrough schedule, representing the marginal impact on destination $\text{PM}_{2.5}$ from a one-unit increase in upwind $\text{PM}_{2.5}$ that is h -hour upwind from the destination. This specification allows us to trace pollution transport dynamics and quantify the contribution of external pollution sources to local $\text{PM}_{2.5}$ levels.

Figure 2 displays the estimated pollution passthrough coefficients from separate regressions for three five-year periods: 2002–2006, 2007–2011, and 2012–2016. For each period, we estimate the

passthrough using all trajectories within that time window. Each line measures the marginal effect of pollution at an upwind location along the trajectory on the local pollution observed at the destination, measured in 6-hour travel time intervals. The general trend reveals that passthrough rates peak within the first one to two days of upwind travel—where a 1 unit increase in upwind PM_{2.5} raises destination levels by approximately 0.25–0.30 units. The effect then declines over longer travel times: at 2–3 days upwind, the marginal impact drops below 0.10, and at even greater distances, it becomes statistically indistinguishable from zero. The detailed results are reported in Table A3, Table A4 and Table A5.

This dynamic pattern quantifies the spatial attenuation of pollution during atmospheric transport, confirming that PM_{2.5} has a pronounced transboundary impact. The findings emphasize that air pollution is rapidly diluted or deposited as it moves away from its source, yet regional spillovers persist over hundreds of kilometers. To give a sense of scale, representative wind speeds of 4 to 6 m/s imply daily travel distances of roughly 345 to 520 kilometers. The straight-line distance between Beijing and Urumqi—the capital city of Xinjiang province, which is the westernmost provincial capital in China—is approximately 2,430 to 2,500 kilometers. At typical wind speeds of 4 to 6 m/s, an air mass would require about 6 to 7 days to travel from Urumqi to Beijing. This magnitude gives a tangible sense of the geographic scale involved in long-range atmospheric transport within China, highlighting the persistence of pollution over extended time and space.

Figure 2: Pollution Passthrough Estimates



Notes: This figure plots the estimated pollution passthrough coefficients based on atmospheric backward trajectory data. Each point reflects the estimated impact of pollution at a specific travel-time distance from the receptor, measured in 6-hour intervals along the backward trajectory. For instance, the 8th interval corresponds to air masses that were located approximately 2 days upwind before reaching the receptor. Lines show estimates by different period—2002–2006 (red), 2007–2011 (blue), and 2012–2016 (green)—with shaded bands denoting confidence intervals. The declining pattern shows how pollution dissipates as travel time increases, indicating the spatial decay of PM_{2.5} transport.

Another observation is the consistency of passthrough functions across different years. As illustrated in the figure, the estimated pollution passthrough patterns remain remarkably similar over time, with only modest variation in magnitude and shape. This suggests that the underlying processes governing pollution transport and dilution have been stable, even as emission levels and regulatory environments may have changed.

To quantify the share of transboundary PM_{2.5} inflows relative to local pollution, we calculate the pollution inflow m_{ij} from an external grid j to a receptor grid i using the following formula::

$$m_{ij} = \sum_{h=1}^{28} \beta_h \times \mathbb{P}_{ijh} \times \text{PM}_{2.5j}.$$

We construct these inflow measures separately for each five-year period from 2002-2017. In this formula, β_h measures the pollution passthrough rate at different travel time intervals h , estimated for each period as described above. Intuitively, β_h captures how effectively pollution is transmitted from an upwind location to the receptor due to distance and atmospheric conditions. \mathbb{P}_{ijh} represents the probability that an air mass passing through location j at h -hour upwind ultimately arrives at

the receptor i , calculated using all trajectories within each five-year window. This is computed as:

$$\mathbb{P}_{ijh} = \frac{T_{ijh}}{T_j},$$

where T_{ijh} represents the frequency of particle trajectories at interval h passing through location j that eventually reach i , while T_j captures the total occurrences of particle trajectories passing through location j . These frequency is calculated using all the trajectories within each five-year period. Thus, \mathbb{P}_{ijh} captures the relative likelihood of pollution transport paths linking sender j to receptor i at a given travel time. Finally, the contribution also depends on $\text{PM}_{2.5j}$ at sender location j . Heavily polluted source regions naturally have a greater potential to influence downwind receptors. Together, this framework combines the physical transmission capability, the transport pathway probability, and the pollution intensity at the source to construct a measure of trans-boundary pollution inflows to any given location.

We aggregate these grid-level transmission intensities to the province level by summing over grids in the receptor province n and the source province i :

$$s_{ni} = \sum_{k \in n} \sum_{j \in i} m_{kj},$$

where s_{ni} represents the total value of pollutant flow from province i to province n .

To obtain province-level pollutant flow shares, we use these bilateral pollutant flow values to calculate the shares:

$$S_{ni} = \frac{s_{ni}}{\sum_{i=1}^N s_{ni}},$$

where S_{nj} represents the share of pollutant in province n that comes from province i .

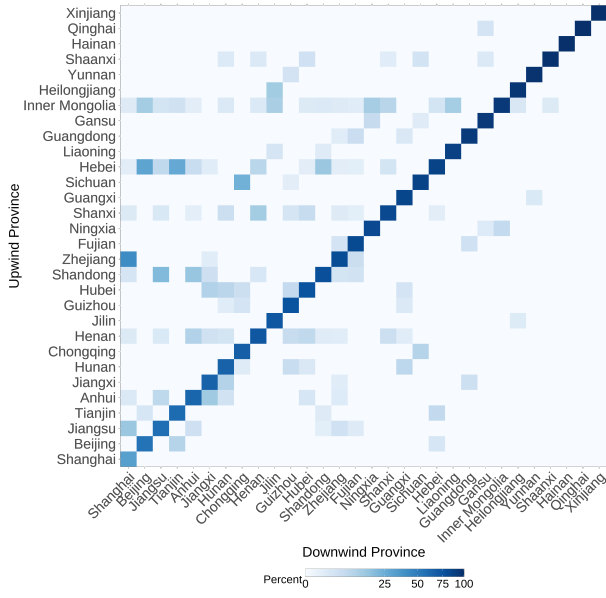
Building on the estimates and method above, we construct a bilateral pollutant-flow matrix that records the share of pollutant from the source province that reaches the receptor. In what follows, we introduce this matrix and highlight its key features to illuminate how transboundary air pollution operates across China.

3.2 Pattern I: Transboundary inflows contribute unevenly to local pollution

Figure 3 displays the bilateral pollutant-flow matrix across Chinese provinces for the year 2017, offering a detailed snapshot of how $\text{PM}_{2.5}$ burdens are assembled from both local and transboundary sources. Rows correspond to source provinces and columns to receptor provinces, tracing the origin and destination of pollution flows. Several features stand out. First, local retention of pollution is highly heterogeneous across regions. The diagonal gradient reveals variations in the share of $\text{PM}_{2.5}$ attributable to own-province emissions, with places like Xinjiang and Ningxia that $\text{PM}_{2.5}$ levels are largely driven by their own emissions, while others are far more exposed to imported pollutants. Second, prominent off-diagonal bands highlight the backbone of China's transboundary transport network: a limited set of upwind–downwind linkages channel pollution from interior and northern

provinces—such as Inner Mongolia and Shanxi—toward populous economic centers, notably the Beijing–Tianjin–Hebei region and the Yangtze River Delta. Finally, the matrix points to a network that is at once sparse and intensely concentrated. Most province-to-province flows are small, yet a handful of highly trafficked corridors account for the primary share of cross-provincial transmission. This stark concentration underscores a key policy insight: targeting interventions at a relatively small number of upwind check-point provinces could disproportionately reduce aggregate downwind pollution exposure, efficiently leveraging spatial structure to maximize health and welfare gains.

Figure 3: Bilateral Pollutant Transport Matrix in 2017



Notes: This figure plots the bilateral pollutant transport matrix across Chinese provinces for the years 2017. The rows represent the source provinces and the columns represent the receptor provinces. The diagonal cells measure the share of locally generated pollution that remains within the same province, while the off-diagonal cells capture cross-province transmission. Darker colors indicate a higher contribution share. The provinces are ordered by the diagonal values.

To fix ideas, we zoom in on two megacities—Beijing and Shanghai. Figures 4 plot each city’s inflow share of PM_{2.5} and map the geographic distribution of upwind provincial contributors. The right panel shows that Beijing receives significant pollution inflows from northern China, with Hebei Province as a major contributor due to its heavy industries. Additionally, arid regions to the northwest of Beijing also contribute substantial pollutant inflows, which aligns with the frequent sandstorms originating from Inner Mongolia that affect the city annually. The left panel shows that Shanghai’s pollution inflow is concentrated within the Yangtze River Delta region, with contributions primarily from neighbouring provinces such as Jiangsu and Zhejiang. Similar to Beijing, Shanghai also receives long-range transported pollution from northern China.

Taken together, these cross-sectional patterns indicate sharp spatial differences in exposure to transboundary air pollution and point to a handful of inter-provincial routes where pollutant transmission is prevalent.

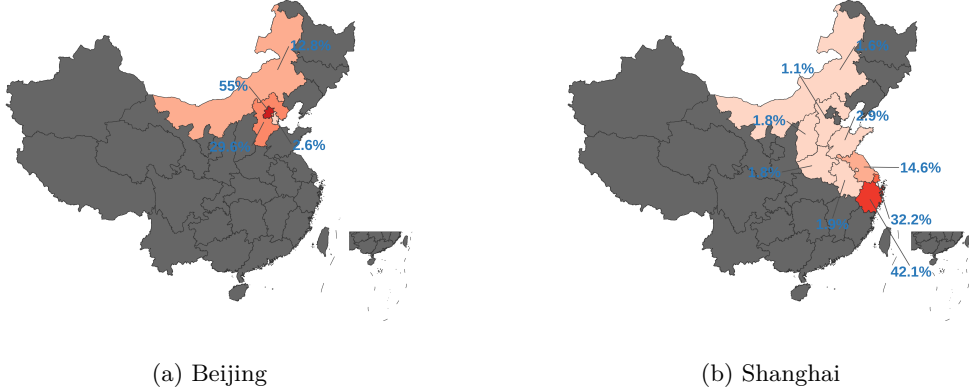


Figure 4: pollutant-flow Share of Beijing and Shanghai

Notes: The maps show, for Beijing and Shanghai, the provincial breakdown of the shares of ambient PM_{2.5} originating from each province. The color gradient represents the degree of pollution contribution, with darker shades indicating higher pollutant inflow from a given region. Areas in grey indicate provinces contributing essentially no PM_{2.5} to the destination province. Beijing's exposure is mainly local plus inflows from Hebei and Inner Mongolia; Shanghai receives transboundary inflows mostly from neighbouring province—Zhejiang and Jiangsu.

3.3 Pattern II: Bilateral flow network is relatively stable over time

A second important question is how frequently and to what extent the prevailing wind patterns change. If the wind regime shifts rapidly and substantially, the established upwind-downwind connections would be unstable, causing policies based on a fixed spatial pollution pattern to become quickly outdated. This volatility would make it much more difficult to effectively target pollution sources or design equitable cross-regional compensation mechanisms compared to a scenario with stable and persistent pollution flows.

Figure A1 illustrates the bilateral pollutant-flow matrices for the years 2002, 2007, 2012, and 2017. The diagonal elements indicate the share of pollution that originates and remains within the same province, while the off-diagonal cells capture cross-province pollution spillovers. Off-diagonal intensity grows gradually over time, indicating more pronounced cross-province transport by 2017. At the same time, the pattern of linkages changes little: similar transmission corridors show up in all figures. In particular, strong upwind-to-downwind connections occur from northern and inland sources toward eastern regions; for example, from Inner Mongolia to Beijing–Tianjin–Hebei, from Hebei to its neighboring provinces, and from Shandong to the Yangtze River Delta (Shanghai–Jiangsu–Zhejiang). Figure A2, which visualizes cross-provincial pollutant transport for sources contributing more than 5% to the destination, reveals a similar pattern. The core structure is remarkably stable between 2010 and 2015: dominant flows run from upwind northern/inland sources toward the North China Plain and the Yangtze River Delta on the eastern coast. These persistent links, alongside generally high local retention, suggest a stable backbone of transboundary transport with growing intensity. The stability is important for policy design: coordination targeted

at the durable upwind sources and major corridors is likely to remain relevant over time, even as the overall extent of cross-boundary dispersion increases.

Table 1: Temporal stability of bilateral pollutant flow matrices

Period	Overall Correlation	Off-diagonal Correlation
2017 & 2012	0.978	0.732
2012 & 2007	0.983	0.728
2007 & 2002	0.981	0.650

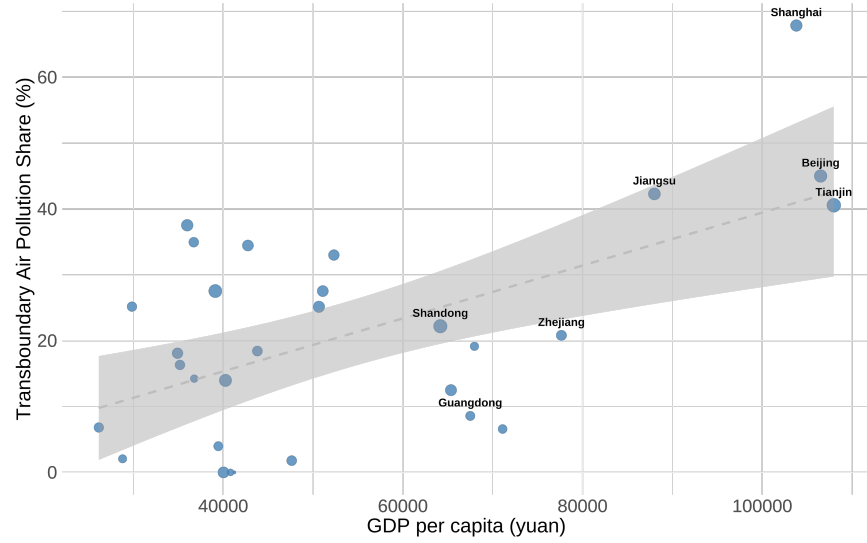
Notes: This table reports the correlation of the bilateral pollutant-flow matrices at five-year intervals. The overall correlation measures the correlation using all matrix entries, while the Off-diagonal correlation excludes within-province elements, capturing only interprovincial pollutant transport patterns.

Table 1 examines the temporal stability of the bilateral pollutant-flow matrices across adjacent five-year windows. Overall correlations are very high indicating that the full spatial pattern of dispersion changes little over time. Off-diagonal correlations, which isolate interprovincial transport, are also substantial, showing persistent cross-boundary corridors with modest variation. Overall, these evidence points to an intensifying yet geographically stable dispersion system, implying that policies targeting persistent upwind sources and a small set of transport corridors are both warranted and likely to remain effective over time.

3.4 Pattern III: Economically advanced provinces disproportionately receive transboundary pollution

Another question that we explores is who bears the brunt of imported pollution. In China’s spatial economy, richer and more densely populated provinces sit along the coast. These areas could attract not only people but also pollutant from inland areas as implied by the previous patterns. We therefore examine whether a province’s transboundary PM_{2.5} rises with economic development. We show below that it does: economically advanced provinces receive a larger fraction of their PM_{2.5} from upwind regions. The pattern has clear distributional and policy implications—without coordination or compensation, development hubs pay a disproportionate price for pollution from elsewhere.

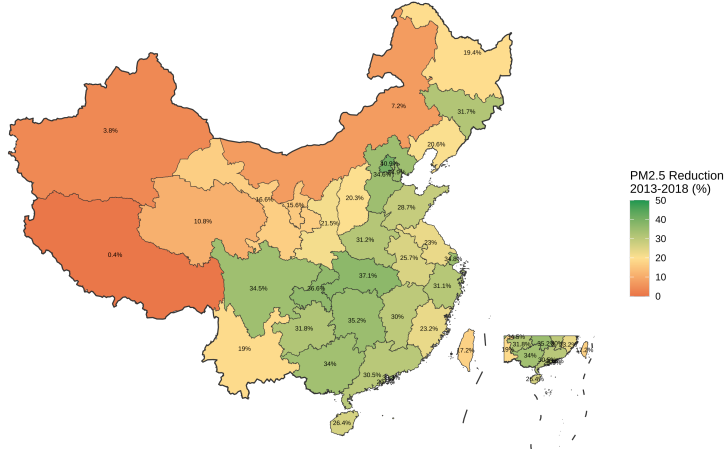
Figure 5: Transboundary Pollution Burden and Economic Development



Notes: This figure relates each province's transboundary PM_{2.5} share (percent of local PM_{2.5} originating outside the province) to GDP per capita. The fitted line slopes upward: richer, coastal provinces receive a larger share of their pollution from upwind regions.

Figure 5 illustrates how the geography of transboundary pollution interacts with economic development. The figure documents a clear positive association between GDP per capita and the transboundary share of local PM_{2.5}. As we move from inland, lower-income regions toward the richer coast, a larger fraction of ambient pollution is imported from upwind neighbors. Megacities (Beijing, Shanghai) and manufacturing hubs (Jiangsu, Zhejiang) sit at the high end of this distribution. This pattern is consistent with geography and atmospheric transport: economically advanced coastal provinces are densely populated receivers located downwind of the northern and northwestern provinces. As a result, a sizable share of pollution exposure in places where many people live and work is determined by emissions produced elsewhere. Figure 6 presents the percentage changes in local PM_{2.5} concentration during China's War on Air Pollution (2013–2018). The figure shows that provinces with larger reductions in PM_{2.5} concentrations are mainly located along the eastern coast and central river basins—areas that are economically advanced and densely populated. Despite receiving substantial inflows of pollution from upwind regions, these provinces achieved some of the largest air-quality improvements nationwide. Taken together, these patterns raise the question of whether transboundary air pollution represents a benefit or a burden. On one hand, emission cuts in upwind regions can deliver large air-quality gains downwind, suggesting potential efficiency gains from coordinated abatement. On the other hand, downwind provinces may bear part of the abatement costs required to mitigate pollution largely generated elsewhere, underscoring the need for inter-jurisdictional cooperation or compensatory mechanisms in environmental policy design.

Figure 6: Provincial PM_{2.5} Reductions during China’s *War on Air Pollution*, 2013–2018



Notes: The map reports the percentage decline in annual mean PM_{2.5} by province from 2013 to 2018; darker green indicates larger reductions and the numbers denote province-level percent changes. Consistent with national evidence of a 40% decline, improvements are highly uneven across space—large in the North China Plain, Yangtze River basin, and parts of the southeast coast, but modest in several western and some northeastern provinces. This spatial heterogeneity motivates the question of how to allocate abatement efficiently when pollution is transported across provincial borders: places that clean up more are not necessarily the ones that generate the largest downwind benefits.

4 Dynamic Quantitative Spatial Model

Building on our empirical findings, we develop an economic geography model that incorporates both physical geography, such as pollution dispersion, and economic geography, including regional trade and migration. The model introduces a central innovation by explicitly incorporating the transport mechanism of air pollution—a factor often overlooked in existing studies but shown by our empirical results to significantly influence local air quality. By modeling the atmospheric movement of pollutants, our framework realistically captures pollution spillovers across geographic boundaries and enables evaluation of how emission control policies shape regional economic outcomes and adaptive responses across space.

4.1 Production and Trade

The production and trade bloc builds on [Caliendo and Parro \(2015\)](#). There are N regions, indexed by n and i , and J sectors in each region, indexed by j and k . In each region, there is a continuum of perfectly competitive firms producing intermediate goods. Firms have a Cobb-Douglas production technology, demanding labour, structures, and materials from all sectors. We introduce pollution and emission tax into production function as in [Taylor and Copeland \(2003\)](#).

Intermediate Goods Producers

We denote the variety of intermediate goods in sector j by $\omega^j \in [0, 1]$. A typical intermediate goods producer makes a two-step decision process to optimize production and maximize profit. In the first step, the producer chooses labour, structure, and sectoral composite goods from all sectors as inputs, and emits pollution e^{nj} as a byproduct. The amount of emissions is subject to the emission tax ψ^{nj} . This emission tax, also called the “pollution tax” or “environmental tax”, represents the overall burden imposed by the environmental regulations. In the second step, the producer diverts part of its potential output into pollution abatement, which reduces its pollution emissions and emission tax duties. In other words, the producer chooses between higher sales and lower tax burdens when making pollution abatement and emission decisions. Combining the two steps (Taylor and Copeland, 2003), the net production function of intermediate goods is given by:

$$q_t^{nj}(\omega^j) = z^{nj}(\omega^j) \left(\left(A_t^{nj} (l_t^{nj}(\omega^j))^{\xi^{nj}} (h_t^{nj}(\omega^j))^{1-\xi^{nj}} \right)^{\gamma^{nj}} \prod_{k=1}^J (m_t^{nj,nk}(\omega^j))^{\gamma^{nj,nk}} \right)^{1-\lambda^j} (e_t^{nj}(\omega^j))^{\lambda^j}$$

where $z^{nj}(\omega^j)$ is producer’s efficiency in producing intermediate good ω^j , A_t^{nj} is the time-varying region-sector specific productivity, $l_t^{nj}(\omega^j)$ is labour input, $h_t^{nj}(\omega^j)$ is structures input, and $m_t^{nj,nk}(\omega^j)$ are composite goods from sector k used to produce one variety of intermediate good in sector j . The parameter ξ^{nj} governs the share of the wage bill in value added; γ^{nj} is the share of value added in the production of sector j and region n ; $\gamma^{nj,nk}$ governs the share of expenditure on composite goods from sector k to produce intermediate good ω^j . We assume that $\sum_k \gamma^{nj,nk} + \gamma^{nj} = 1$ for the constant return to scale technology. The pollution elasticity λ^j is a crucial set of parameters in our model. It is the share of emission tax in the revenue, and it also measures the elasticity of pollution emissions intensity with respect to pollution abatement intensity. By defining pollution emission intensity $EI^{nj} \equiv \frac{e^{nj}}{p^{nj} q^{nj}}$, firms optimise yields:

$$EI^{nj} = \frac{\lambda^j}{\psi^{nj}} \tag{1}$$

where ψ^{nj} is emission tax rate. This is intuitive as the emission intensity will be lower if the pollution elasticity is lower and abatement is thus more effective, or if the emission tax is higher so that producers emit less to reduce the emission tax. This also shows policies will have different effects on emissions in different sectors because sectors are different in their pollution elasticity.

We denote by r_t^{nj} the rental price of structures in market (n, j) . Thus, the unit cost of production takes the following form:

$$x_t^{nj} = \Xi^{nj} \left(\left((w_t^{nj})^{\xi^{nj}} (r_t^{nj})^{1-\xi^{nj}} \right)^{\gamma^{nj}} \prod_{k=1}^J (P_t^{nk})^{\gamma^{nj,nk}} \right)^{1-\lambda^j} (\psi_t^{nj})^{\lambda^j} \tag{2}$$

where Ξ^{nj} is a constant and P_t^{nj} is the price of materials in production.

Trade is subject to bilateral iceberg costs $\kappa_t^{nj,ij}$. One unit of any variety of intermediate good j shipped from region i to region n requires producing $\kappa_t^{nj,ij} \geq 1$ units in region i . Following Eaton

and Kortum (2002), we assume that the efficiency of an intermediate good producer $z^{nj}(\omega^j)$ follows a Fréchet distribution with shape parameter θ^j . Thus, the price of intermediate goods of variety ω^j is as follows

$$p_t^{nj}(\omega^j) = \min_i \left\{ \frac{\kappa_t^{nj,ij} x_t^{ij}}{z^{ij}(\omega^j) (A_t^{ij})^{\gamma^{ij}(1-\lambda^{ij})}} \right\}$$

Local Sectoral Aggregate Goods

Local sectoral aggregate goods are used as materials for the production of intermediate goods as well as for final consumption. We denote the quantity of produced aggregate sectoral goods j in region n as Q_t^{nj} , and the quantity demanded of an intermediate good of a given variety from the lowest-cost supplier as $\tilde{q}_t^{nj}(z^j)$. We index varieties from different markets using $z^j = (z^{1j}, z^{2j}, \dots, z^{Nj})$. The production of local sectoral goods is given by

$$Q_t^{nj} = \left(\int (\tilde{q}_t^{nj}(z^j))^{1-1/\eta^{nj}} d\phi^j(z^j) \right)^{\eta^{nj}/(\eta^{nj}-1)}$$

where $\phi^j(z^j) = \exp \left\{ -\sum_{n=1}^N (z^{nj})^{-\theta^j} \right\}$ is the joint distribution over the vector z^j with the marginal distribution given by $\phi^{nj}(z^{nj}) = \exp \left\{ -(z^{nj})^{-\theta^j} \right\}$. Given the properties of the Fréchet distribution, the price of the sectoral aggregate good j in region n at time t is

$$P_t^{nj} = \Gamma(1 + \frac{1 - \eta^{nj}}{\theta^j})^{1/(1-\eta^{nj})} \left(\sum_{i=1}^N \left(\kappa_t^{nj,ij} x_t^{ij} \right)^{-\theta^j} (A_t^{ij})^{\theta^j \gamma^{ij}(1-\lambda^{ij})} \right)^{-1/\theta^j} \quad (3)$$

Then equilibrium trade shares, the fraction of total expenditure in market nj on goods from market ij , are

$$\pi_t^{nj,ij} = \frac{\left(\kappa_t^{nj,ij} x_t^{ij} \right)^{-\theta^j} (A_t^{ij})^{\theta^j \gamma^{ij}(1-\lambda^{ij})}}{\sum_{m=1}^N \left(\kappa_t^{nj,mj} x_t^{mj} \right)^{-\theta^j} (A_t^{mj})^{\theta^j \gamma^{mj}(1-\lambda^{mj})}} \quad (4)$$

4.2 Consumption and Migration

The consumption and migration bloc builds on Caliendo and Parro (2022). The preferences of a representative household in location n are defined over goods and local amenity:

$$U_t^n = \log B_t^n C_t^n = \log B_t^n \prod_{k=1}^J (C_t^{nk})^{\alpha^k}$$

where C_t^{nk} is the consumption of sector k goods in location n at time t and α^k is the final consumption share, with $\sum_{k=1}^J \alpha^k = 1$. B_t^n is local amenity of location n at time t . The consumer price index is therefore $P_t^n = \prod_j \left(\frac{P_t^{nj}}{\alpha^j} \right)^{\alpha^j}$, where P_t^{nj} is the price of composite goods from region n and sector j . Denote regional total income as I_t^{nj} . Thus we have $C_t^{nj} = I_t^{nj} / (P_t^n L_t^{nj})$. In each

region-sector combination nj , there is a competitive labour market. Household supplies a unit of labour inelastically and receives a competitive market wage w_t^{nj} .

The household problem is dynamic. Workers are freely mobile across sectors but costly across regions subject to a migration cost $\tau^{n,i}$, from region n to region i . The lifetime utility is given by

$$v_t^n = \log B_t^n C_t^n + \max_{\{i\}_{i=1}^N} \{\beta E[v_{t+1}^i] - \tau^{n,i} + \nu \epsilon_t^i\}$$

where v_t^n is the lifetime utility of a household currently in region n at time t and the expectation is taken over future realisations of the idiosyncratic shock. The parameter ν scales the variance of the idiosyncratic shocks.

We assume that the idiosyncratic shock ϵ_t^i is i.i.d. over time and follows Type-I Extreme Value distribution with zero mean. In particular, $F(\epsilon) = \exp(-\exp(-\epsilon - \bar{\gamma}))$, where $\bar{\gamma} \equiv \int_{-\infty}^{\infty} x \exp(-x - \exp(-x)) dx$ is Euler's constant and $f(\epsilon) = \partial F / \partial \epsilon$.

Denote $V_t^n = E(v_t^n)$. Based on the above assumption, we can obtain

$$V_t^n = \log \frac{B_t^n I_t^n}{P_t^n L_t^n} + \nu \log \left(\sum_{i=1}^N \exp (\beta V_{t+1}^i - \tau^{n,i})^{\frac{1}{\nu}} \right) \quad (5)$$

We denote $\mu_t^{n,i}$ the fraction of households that relocate from location n to location i . Then the equilibrium migration share is

$$\mu_t^{n,i} = \frac{\exp (\beta V_{t+1}^i - \tau^{n,i})^{1/\nu}}{\sum_{m=1}^N \exp (\beta V_{t+1}^m - \tau^{n,m})^{1/\nu}} \quad (6)$$

Define $Y_{t+1}^n = \exp(V_{t+1}^n - V_t^n)^{\frac{1}{\nu}}$, then we can rewrite equations (5) and (6) as

$$Y_{t+1}^n = \left(\frac{B_{t+1}^n I_{t+1}^n P_t^n L_t^n}{B_t^n I_t^n P_{t+1}^n L_{t+1}^n} \right)^{\frac{1}{\nu}} \left(\sum_{i=1}^N \mu_t^{n,i} (Y_{t+2}^i)^{\beta} \right) \quad (7)$$

$$\frac{\mu_{t+1}^{n,i}}{\mu_t^{n,i}} = \frac{(Y_{t+2}^i)^{\beta}}{\sum_{m=1}^N \mu_t^{n,m} (Y_{t+2}^m)^{\beta}} \quad (8)$$

The distribution of labour across markets is

$$L_{t+1}^n = \sum_{i=1}^N \mu_t^{i,n} L_t^i \quad (9)$$

4.3 Pollution and Dispersion

In this section, we outline how the distribution of air pollutants is determined in each period and proceed to define the damage function. Following the atmospheric science literature, we model air pollution dynamics as comprising both local deposition and spatial dispersion across regions. This formulation captures the dual nature of pollutant behaviour: some portion of pollutant is absorbed or settles near the source, while the remainder is transported through the atmosphere to downwind

locations. By incorporating both mechanisms, the model provides a simple yet realistic framework to study the environmental and economic consequences of both localized pollution exposure and transboundary pollution spillovers.

Firms make production and emission decisions in each period as described above. The total emissions generated in location n at time t are defined as $e_t^n = \sum_j e_t^{nj}$. Let E_t^n denote the pollutant stock at the beginning of period t . The pollutant stock at the end of period t , before dispersion occurs, is denoted as \bar{E}_t^n . We use ρ to denote the pollutant-flow matrix, where $\rho^{n,i}$ represents the share of pollutants in location i that arrives in location n .

We model the pollutant dynamics within each period as a two-stage process, comprising local deposition followed by spatial dispersion across regions. The stock of airborne pollutants after local deposition, denoted by \bar{E}_t^n , evolves from the existing pollutant stock E_t^n and new emissions e_t^n according to:

$$\bar{E}_t^n = (1 - \delta)E_t^n + e_t^n, \quad (10)$$

where δ is the deposition rate, representing the fraction of pollutants that are removed locally through dry and wet processes. The airborne pollutants \bar{E}_t^n are then subject to atmospheric transport, and the spatial redistribution across regions is governed by the following law of motion:

$$E_{t+1}^n = \sum_{i=1}^N \rho^{n,i} \bar{E}_t^i. \quad (11)$$

This structure enables us to separately model local environmental cleansing and interregional pollutant spillovers. We calibrate the transmission matrix ρ using air trajectory data, following the methodology detailed in Section 3. We calibrate the δ in Section 5.6.

Finally, we introduce pollution externality. We allow the amenity, B_t^n , and productivity, A_t^{nj} , to depend on constant fundamentals and pollution externality. We first define the concentration of location n at time t can be expressed as:

$$con_t^n = \frac{E_t^n}{V^n}, \quad (12)$$

where V^n denotes the atmospheric volume over province n . Following standard atmospheric modeling conventions, we calculate volume as $V^n = \text{Area}^n \times H$, where Area^n is the provincial land area and H is the mixing height, which we set at 1,000 meters-a typical value for the planetary boundary layer where most PM_{2.5} concentrates.

Local amenity can be affected governed by the following function:

$$B_t^n = \bar{B}^n (con_t^n)^{\eta_b} \quad (13)$$

This shows that high pollution reduces amenity which in turn deters workers from migrating to that region. This not only affect household utility directly, but also affect the production by changing

labour allocation. Secondly, local sectoral productivity can also be affected by pollution:

$$A_t^{nj} = \bar{A}^{nj} (con_t^n)^{\eta_a^j} \quad (14)$$

This shows that high pollution reduces productivity in different sectors which affect production and local wage directly.

4.4 Competitive Equilibrium

We solve the model and characterise the equilibrium of the model. Let X_t^{nj} be the total expenditure on goods from sector j region n . Then, goods market clearing implies total output in each region-sector equals total demand of input used in production in all other region-sectors and final demand in region n

$$X_t^{nj} = \sum_{k=1}^J (1 - \lambda^k) \gamma^{nk,nj} \sum_{i=1}^N \pi_t^{ik,nk} X_t^{ik} + \alpha^j I_t^n \quad (15)$$

where $I_t^n = w_t^n L_t^n + \sum_k (r_t^{nk} H^{nk} + \psi^{nk} e_t^{nk})$.

Labour market clearing condition is

$$L_t^{nj} = \frac{\gamma^{nj} (1 - \lambda^j) \xi^{nj}}{w_t^n} \sum_i \pi_t^{ij,nj} X_t^{ij} \quad (16)$$

The market clearing for structures in region n and sector j must satisfy

$$H^{nj} = \frac{\gamma^{nj} (1 - \lambda^j) (1 - \xi_{nj})}{r_t^{nj}} \sum_i \pi_t^{ij,nj} X_t^{ij} \quad (17)$$

Optimal Emission by firm is given by

$$e_t^{nj} = \frac{\lambda^j}{\psi^{nj}} \sum_i \pi_t^{ij,nj} X_t^{ij} \quad (18)$$

The fundamentals of the economy are deterministic, some time varying and some constant. The time-varying fundamentals of the economy are productivity $A_t = \{A_t^{nj}\}_{n=1,j=1}^{N,J}$, local amenity $B_t = \{B_t^n\}_{n=1}^N$, bilateral trade cost $K_t = \{\kappa_t^{nj,ij}\}_{n=1,i=1,j=1}^{N,N,J}$, and emission tax rate $\Psi_t = \{\psi_t^{nj}\}_{n=1,j=0}^{N,J}$. We denote $\Theta_t \equiv (A_t, B_t, K_t, \Psi_t)$. Constant fundamentals are the labour relocation costs $\tau = \{\tau^{n,i}\}_{n=1,i=1}^{N,N}$ and the stock of structures across markets $H = \{H^{nj}\}_{n=1,j=1}^{N,J}$. We denote $\bar{\Theta} \equiv (\tau, H)$. The parameters in our model, assumed constant throughout the paper, are given by the value added shares (γ^{nj}); the labour shares in value added (ξ^{nj}); the input-output coefficients ($\gamma^{nk,nj}$); the emission tax shares (λ^j); the final consumption expenditure shares (α^j); the discount factor (β); the trade elasticity (θ^j); and the migration elasticity (ν); and the correlation matrix ρ .

Equilibrium of the Dynamic Spatial Model. Given an initial distribution of workers $\{L_0^{nj}\}_{n=1,j=1}^{N,J}$, initial pollutantion level $\{\bar{E}_0^n\}_{n=1}^N$ and an endowment of structures, $H = \{H^{nj}\}_{n=1,j=1}^{N,J}$, a path of

fundamentals $\{\bar{A}^{nj}, \bar{B}^n, \kappa_t^{nj,ij}, \tau_t^{n,i}, \psi_t^{nj}\}_{n=1,j=1,t=0}^{N,J,\infty}$, parameters $\{\gamma^{nj}, \xi^{nj}, \gamma^{nk,nj}, \lambda^j, \alpha^j\}$, the discount factor (β), trade elasticity $\{\theta^j\}_{j=1}^J$, migration elasticity ν and correlation matrix ρ , a sequential competitive equilibrium of the dynamic spatial model is characterised by a sequence of wage $\{w_t^{nj}\}_{n=1,j=1,t=0}^{N,J,\infty}$ such that the following conditions are satisfied:

- Goods market clearing condition satisfies equation (15) in each period.
- Labour market clearing condition satisfies equation (16) in each period.
- Structure price is given by the structure clearing condition (17) in each period.
- Optimal emission in each period is given by equation (18) in each period.
- Amenity and productivity is given by equation (13) and (14) respectively in each period.
- Law of motion for labour is given by equation (9) and (6).
- Expected value is given by (5).
- Law of motion for air pollution is given by equation (10) and (11).

4.5 Aggregate Welfare

It can be shown that the expected lifetime utility of location n at time t is given by:

$$V_t^n = \sum_{s=t}^{\infty} \beta^{s-t} \log \frac{B_s^n \times I_s^n}{(\mu_s^{n,n})^\nu \times P_s^n L_s^n}$$

This welfare measure may vary across locations. Welfare is aggregated across provinces in China using a utilitarian approach which captures the mean welfare across all provinces weighted by their respective initial population share:

$$W_t = \sum_{n \in N} \frac{L_0^n}{\sum_{i \in N} L_0^i} \left\{ \sum_{s=t}^{\infty} \beta^{s-t} \log \left(\frac{B_s^n I_s^n}{(\mu_s^{n,n})^\nu P_s^n L_s^n} \right) \right\}$$

5 Model Parameterization and Calibration

This section describes parameterization of the model and uses these parameters together with the data described in Section 2 and the model's equilibrium conditions to calibrate values across Chinese provinces starting from 2000. We focus our analysis on 30 Chinese provinces. We exclude Tibet, Hongkong, Macao and Taiwan due to data limitation.

5.1 Factor shares and input-output linkage

The share of wage bill in value added ξ^{nj} , share of value added in total output γ^{nj} and share of intermediate input in total output $\gamma^{nj,nk}$ are calculated using the 2002 Chinese Regional Input-Output Table. The dataset provides information on labour compensation, intermediate input, value added, total output by industry for each province in China. We calculate these factor shares and input-output linkages at the provincial level.

5.2 Emission elasticity and emission tax

The emission elasticity λ^j captures the responsiveness of emission with respect to abatement. We calibrate λ^j using equation (1), which relates emission productivity—defined as gross output per unit of emissions—to the emission tax and emission elasticity:

$$\frac{\text{GO}^{nj}}{e^{nj}} = \frac{\psi^{nj}}{\lambda^j},$$

where GO^{nj} denotes gross output, e^{nj} denotes emissions, and ψ^{nj} represents the emission tax rate. This equation implies that emission productivity depends jointly on the emission elasticity and emission tax rate. Following [Wang, Wang and Xie \(2024\)](#), we calibrate λ^j and ψ^{nj} to match emission productivity across all region-sector pairs in China. To separate λ^j from ψ^{nj} , we take the average across all regions, yielding the sector-specific condition for any sector j :

$$\frac{1}{N} \sum_{n=1}^N \frac{\text{GO}^{nj}}{e^{nj}} = \frac{1}{\lambda^j} \times \frac{1}{N} \sum_{n=1}^N \psi^{nj}.$$

We assume that all the observed variations in emission productivity across sectors are mainly driven by difference in technology (i.e λ^j) rather than emission tax. Accordingly, we normalise $\frac{1}{N} \sum_{n=1}^N \psi^{nj} = 1$ for all j . The final calibrated values of λ^j are presented in Table 2.

To provide a benchmark for our estimates, we apply an identical methodology to U.S. manufacturing sector in the year 2000, yielding an emission elasticity estimate of 0.023. This value is consistent with, though somewhat higher than, the estimate of 0.011 reported in [Shapiro and Walker \(2018\)](#).

Table 2: Sectoral emission elasticity

λ^j	Value
Agriculture	0.0061
Manufacturing	0.0058
Service	0.0122

5.3 Trade elasticity

We adopt the sector-level trade elasticity estimates from [Caliendo and Parro \(2015\)](#). Specifically, we calibrate the trade elasticity for agriculture at 8.11 and for manufacturing at 4.55, corresponding to

the aggregate estimates reported in their study. The service sector is assumed to be non-tradable.

5.4 Migration elasticity

We calibrate the migration elasticity ($\frac{1}{\nu}$) to the value in [Tombe and Zhu \(2019\)](#), which yields a value of 1.5.

5.5 Elasticity of substitution and discount factor

We set the elasticity of substitution as in [Desmet, Nagy and Rossi-Hansberg \(2018\)](#), which yield a value of 2. Given that the model is calibrated at five-year intervals, the discount factor β is expressed on a five-year basis. In line with standard practice in the evaluation of long-term public investments and climate policy, we adopt an annual discount rate of 2%, consistent with values commonly used in the literature. This choice implies a five-year discount factor of approximately 0.91, which is employed as the central parameter in the baseline simulations.

5.6 Deposition rate

Our model treats pollution E_t^n as a stock variable that evolves through emission, transport, and deposition. The deposition rate δ , the fraction of airborne PM_{2.5} that settles or is removed from the atmosphere each period, governs how quickly pollution dissipates and thus shapes the severity of transboundary externalities. Atmospheric science provides rough bounds: surface-layer PM_{2.5} deposits through gravitational settling, dry deposition to vegetation and surfaces, and wet removal through precipitation, with typical residence times of days to weeks ([Pleim et al., 2022](#); [Zhang et al., 2018](#)). However, translating these physical processes to our five-year model periods requires empirical discipline. Rather than impose an ad-hoc deposition parameter, we estimate δ directly by fitting the model's pollution dynamics to observed concentration trajectories.

We use the PM_{2.5} concentration data from [Van Donkelaar et al. \(2021\)](#) and PM_{2.5} emission data from [Crippa et al. \(2020\)](#) to discipline our calibration. Our model tracks pollution stocks E_t^n , the mass of PM_{2.5} suspended in each province's air column, while observations come in two forms: satellite-derived concentrations $con_t(\mu\text{g}/\text{m}^3)$ and emission inventories e_t (tons per year). Converting concentration to stock requires multiplying by mixing volume: $E_t \approx con_t \times V$, where $V = \text{Area} \times H$ and H is the atmospheric mixing height which we set at 1000 meters. Therefore, given equation (10) and (11), we first calculate the model predicts concentration evolution as:

$$con_{t+1}^n = \frac{1}{V^n} \left(\sum_n \rho_t^{n,i} (1 - \delta) V^i con_t^i + k_e e_t^i \right)$$

The coefficient k_e serves as a scaling factor that reconciles unit and measurement differences between emission data and concentrations data. We choose (δ, k_e) to minimize the sum of squared log deviations between predicted and observed concentrations across all provinces and three five-year intervals:

$$\min_{\delta, k_e} \sum_t \sum_n \left[\log c_{t+1}^n(\delta, k_e) - \log c_{t+1}^{n,\text{obs}} \right]^2.$$

The calibration yields $\delta = 0.16$. Figure 7 plots predicted versus observed concentrations across all province-year pairs. Most points cluster near the 45° line, indicating that the calibrated parameters reproduce the level and cross-sectional variation of concentrations reasonably well. Deviations reflect residual measurement noise and unmodeled heterogeneity

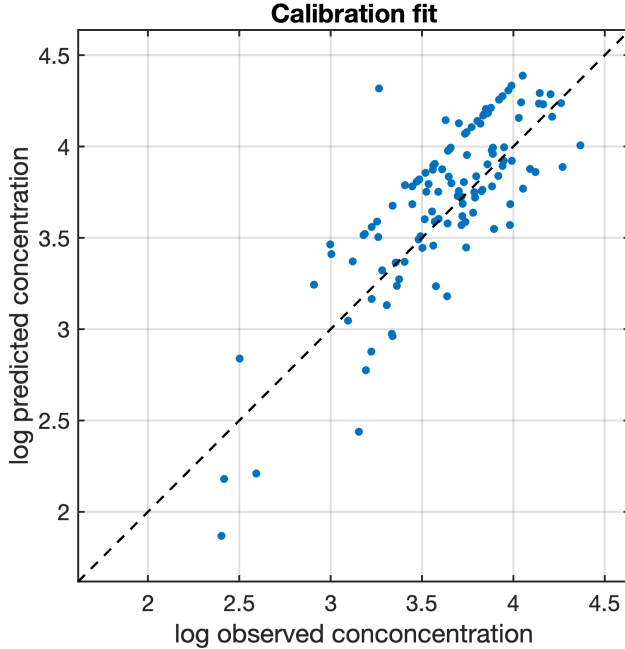


Figure 7: Observed concentration vs. model-implied concentration

Notes: This figure plots model-predicted versus observed PM_{2.5} concentrations on log scales. Each dot is a province-period observation. Most points cluster near the 45° line, indicating that the calibrated parameters reproduce the level and cross-sectional variation of concentrations reasonably well; deviations reflect residual measurement noise and unmodeled heterogeneity.

5.7 Calibrate province-level productivity and amenity

Using the data described above and the parameters calibrated in the preceding subsections, the model is used to infer relative productivities and amenities across prefectures such that the observed allocation corresponds to an equilibrium outcome in the initial period. The procedures for recovering productivity and amenity are outlined in Appendix 3 and Appendix 4. The model-inverted values are presented in Figure A3. The recovered fundamentals line up with well-known geographic patterns in China. The model-inverted productivity—value-added-weighted average of sectoral productivities—is highest in the major coastal city regions, remains elevated along the Yangtze corridor and a few inland hubs, and is markedly lower across the western interior and the far northwest. This mirrors the observed concentration manufacturing hubs in coastal provinces,

with thinner markets and higher trade frictions inland. The inverted amenity displays a complementary geography: higher values in temperate, economically vibrant coastal provinces and in a few livable basins (e.g., the Sichuan–Chongqing area), and lower values in the arid north/northwest and in heavy-industry belts. This is consistent with differences in climate, pollution exposure, urban services, and public goods that attract migrants and sustain higher willingness-to-pay in large coastal cities. Taken together, the spatial gradients in the model-implied productivity and amenity are plausible and align with widely documented urbanization and development patterns, giving face validity to the inversion.

5.8 Calibrate trade cost

We calibrate trade costs by matching the observed regional trade data. Using equation 4, we can have following equation,

$$\frac{\pi_t^{ij,nj}}{\pi_t^{ij,ij}} \frac{\pi_t^{nj,ij}}{\pi_t^{nj,nj}} = \left(\kappa_t^{ij,nj} \right)^{-2\theta^j}.$$

Regional trade flow is obtained from provincial input-output data.

5.9 Calibrate migration cost

We calibrate migration costs by matching the observed migration shares in the data. In the model, we have

$$\frac{\mu_t^{n,i} \mu_t^{i,n}}{\mu_t^{n,n} \mu_t^{i,i}} = \exp \left(2\tau^{n,i} \right)^{-1/\nu}.$$

We determine the migration costs by ensuring that the model-implied migration shares align with those observed in the data.

5.10 Estimate damage coefficient

Air pollution has impact on productivity and amenity. From equation (14) and (13), we have following equations:

$$\begin{aligned} \log A_{it}^j &= \delta_i^j + \eta_a^j \log(\text{con}_{it}) \\ \log B_{it} &= \gamma_i + \eta_b \log(\text{con}_{it}) \end{aligned}$$

where i indexes provinces, j sectors, and t years; c_{it} denotes local PM_{2.5} concentration in province i at time t ; δ_i^j and γ_i are time-invariant fundamentals capturing baseline productivity and amenity; and η_a^j and η_b are the elasticities of productivity and amenity with respect to pollution.

A simple OLS regression of above equations yields biased estimates because local concentration is endogenous. Local PM_{2.5} concentrations are correlated with unobserved factors that also affect productivity and amenity. As a result, OLS estimates are subject to reverse causality and omitted variable bias. To identify causal effects, we follow the literature and instrument for local pollution using thermal inversions. A thermal inversion is a meteorological condition under which a warm

air layer overlays cooler air near the surface, suppressing vertical mixing and trapping pollutants. Thermal inversion can affect local air quality because inversions mechanically impede pollutant dispersion, producing sharp spikes in local concentrations. This IV is widely used in the empirical literature studying the economic impact of air pollution (Khanna et al., 2021; Chen, Oliva and Zhang, 2022; Fu, Viard and Zhang, 2021). We follow the literature to calculate the average strength of thermal inversions over each five-year period. Thermal inversion strength is defined using above-ground temperature minus ground temperature. A positive difference indicates the existence of a thermal inversion and the magnitude measures the inversion strength.

The results from first-stage and IV regression are presented in Table A1 and A2. The results from the first-stage regression suggest that a 1 percentage increase in average thermal inversion strength leads to a 0.11 percent increase in PM_{2.5}, which is close to estimate of 0.3 in Chen, Oliva and Zhang (2022). The 2SLS IV estimates reveal heterogeneous sectoral effects: the agricultural sector experiences the largest negative impact, while indoor economic activities are less affected. The results also show negatively impact on amenity. It is worth noting that while several empirical studies estimate the impact of air pollution on productivity, their results are not directly comparable due to differences in how productivity is measured, as well as variations between short-run and long-run effects.

5.11 Calibrate source-oriented bilateral pollutant-flow share $\{\rho^{ni}\}_{n=1,i=i}^{N,N}$

We calibrate the bilateral pollutant-flow share ρ^{ni} following the procedure in Section 3, with one adjustment for model compatibility. In the empirical section, we estimate receptor-oriented shares—the fraction of pollution in province n originating from source i . However, the model requires source-oriented shares ρ^{ni} , representing the portion of pollutant in province i that travel to province n , as specified in equation (11). We therefore convert the empirical estimates into source-normalized shares before implementing them in the quantitative framework.

The calibration proceeds in three steps. First, we compute the grid-level transmission intensity between source grid j and receptor grid i as:

$$f_{ij} = \sum_{h=1}^{28} \beta_h \cdot \mathbb{P}_{ijh} \cdot \text{PM}_{2.5,j},$$

where β_h denotes the pass-through rate of pollutants from h hours upwind, \mathbb{P}_{ijh} is the trajectory probability that air parcel transits j at h hours before reaching i , and $\text{PM}_{2.5,j}$ is the particulate matter concentration in grid j .

Next, we aggregate grid-level flows to construct a province-to-province transmission matrix:

$$F_{ni} = \sum_{k \in n} \sum_{j \in i} f_{kj},$$

where the outer sums are taken over all grids in destination province n and origin province i ,

respectively. This aggregation is performed separately for each five-year period (2002-2006, 2007-2011, and 2012-2017) to capture temporal variation in atmospheric transport patterns.

Finally, we normalize the aggregated flows to obtain the source-oriented transport share matrix $\{\rho^{ni}\}_{n=1,i=i}^{N,N}$, which is used in the dynamic spatial equilibrium model:

$$\rho^{ni} = \frac{F_{ni}}{\sum_n F_{ni}}.$$

This normalization ensures $\sum_{n=1}^N \rho^{ni} = 1$, representing the fraction of pollutants emitted in province i that is deposited in province n within the modeling period. The resulting bilateral flow matrix provides a quantitative basis for simulating transboundary pollution externalities and evaluating spatially targeted regulatory policies.

6 The Welfare and Policy Incidence of Transboundary Air Pollution

In this section we use the calibrated model and ask a simple question: to what extent does transboundary air pollution shape welfare and incidence? The empirical evidence above documented large and uneven bilateral pollutant flows; here we explore their welfare impact with two complementary exercises. First, we quantify the aggregate welfare consequences of transboundary air pollution. We compare the baseline economy—calibrated to observed cross-provincial pollution flows—to counterfactual scenarios where pollution is progressively localized within provinces of origin. This exercise reveals whether atmospheric transport increases or decreases national welfare by reshuffling pollution across space. Second, we perform a policy gradient decomposition under the calibrated bilateral pollutant-flow structure. This analysis estimates the marginal welfare impact of provincial emissions tax on the spatial economy. It quantifies how increasing the emissions tax in a single province affects overall national welfare.

These two exercises address distinct but complementary questions. The first examines how aggregate and regional welfare vary with the strength of transboundary air pollution under a given emission tax regime. The second explores, conditional on the estimated transboundary pollution structure, how changes in local emission taxes affect welfare both locally and in other regions through pollution dispersion. Together, they provide a nuanced understanding of the welfare implications of transboundary air pollution and the spatial transmission of regulatory policies, laying important groundwork for the policy design analysis that follows.

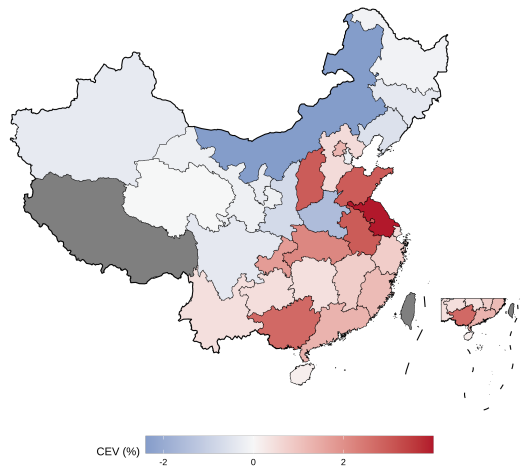
6.1 The Welfare Cost of Transboundary Pollution

Transboundary air pollution creates a fundamental tension. Atmospheric dispersion spreads pollutant from upwind regions to downwind populous regions, potentially magnifying aggregate exposure and damages. Yet the same process can benefit upwind provinces by exporting their pollution burden elsewhere. We quantify the welfare effects of transboundary pollution by comparing two scenarios: a fully localized benchmark where each province's emissions remain entirely local, and

the calibrated transboundary case where pollution disperses according to our estimated transport network. In both scenarios, we hold fixed technologies, preferences and initial conditions. We solve the dynamic spatial equilibrium and calculate consumption-equivalent welfare (CEV) for each province.

The simulated results show that the aggregate welfare cost is substantial. By shutting down the transboundary air pollution channel, national welfare would increase by 1% in consumption-equivalent terms. This cost reflects the spatial spillover effect of air pollution—atmospheric transport carries pollution from inland provinces to densely populated eastern and southeastern regions, degrading air quality where people concentrate. Yet this aggregate cost masks sharp geographic redistribution. Figure 8 shows the spatial distribution of welfare impact. Regions in blue represent those that lose when there is no transboundary air pollution. Removing the pollution export channel would force upwind regions in northern and northwestern China to bear the full cost of the pollution they generate domestically. On the contrary, regions in the east and south benefit when there is no transboundary air pollution. This spatial pattern mirrors the empirical transport corridors documented in Section 3.

Figure 8: Welfare changes from transboundary air pollution



Notes: The map shows the consumption-equivalent welfare (CEV, %) change for each province, contrasting a scenario with no transboundary air pollution against the calibrated baseline with bilateral pollution flows. Fundamentals are held fixed; CEV is computed from lifetime utility and expressed in percent. Red provinces gain from transboundary air pollution, while blue provinces lose.

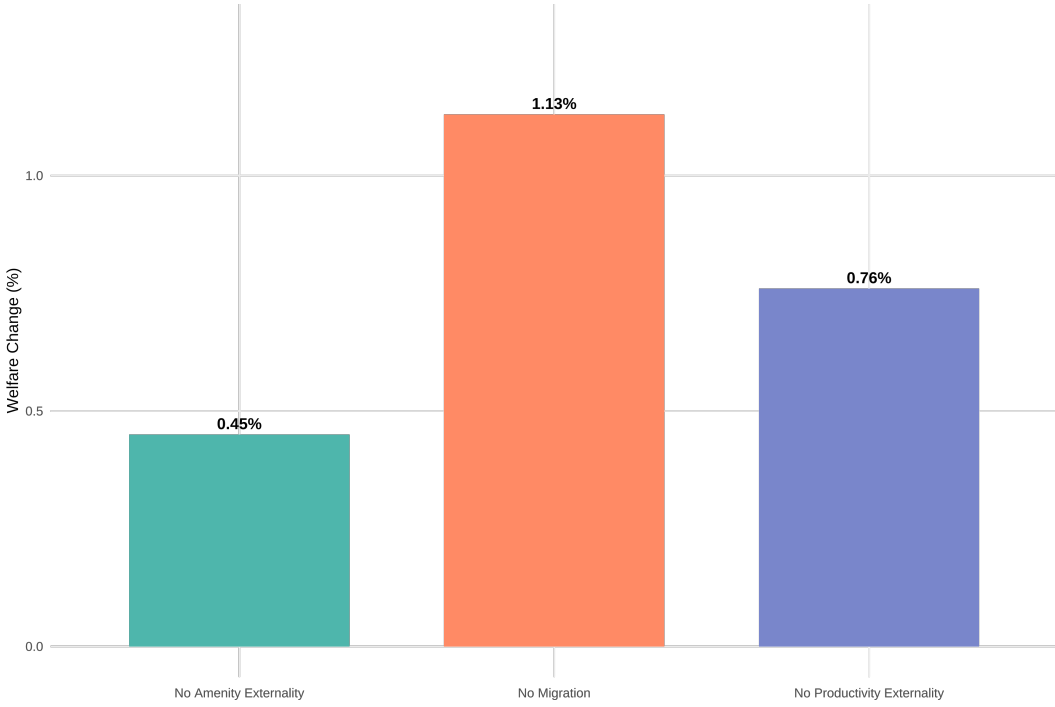
What drives these welfare changes? To isolate the mechanisms through which transboundary pollution affects welfare, we conduct a counterfactual decomposition. We re-solve the model under three alternative scenarios, each shutting down one channel through which pollution affects the economy: amenity, productivity, and migration. Figure 9 reports the aggregate welfare loss from transboundary transport in each scenario, measured as the consumption-equivalent welfare difference between no dispersion and calibrated dispersion.

Amenity effects dominate. In the baseline with all channels active, transboundary transport reduces national welfare by 1%. Shutting down the negative externality effect on amenity reduces the welfare cost to just 0.45%, eliminating 55% of the baseline loss. This indicates that the bulk of transboundary pollution's welfare impact operates through reduced quality of life rather than economic production. Coastal provinces receiving high transboundary inflows suffer primarily from deteriorated air quality, with these amenity losses far exceeding any indirect effects through wages or prices.

Migration responses are limited. When we eliminate migration, the welfare cost rises only slightly to 1.13%, a mere 0.1 percentage points above baseline. This near-zero contribution of migration stands in contrast to city-level evidence showing significant population responses to air quality ([Chen, Oliva and Zhang, 2022](#); [Khanna et al., 2021](#)). The divergence reflects our focus on provinces, the administrative level at which China designs and implements pollution policies. Cross-provincial migration costs are substantially higher than within-province moves, dampening spatial reallocation even when air quality differentials are large. Pollution's welfare effects accrue primarily to existing residents through amenity and consumption channels rather than through population sorting.

Productivity effects are moderate. Shutting down pollution's effect on productivity-so firms' output no longer depends on local air quality-yields a 0.76% welfare cost from transboundary transport, about two-thirds of the baseline. This indicates that pollution's drag on economic output, while meaningful, is secondary to its direct disamenity. The general equilibrium adjustments through production networks and terms of trade contribute roughly one-third of the total welfare impact.

Figure 9: Welfare impact through different channels



Notes: The figure reports the aggregate welfare effects of transboundary pollution, measured as the consumption-equivalent welfare difference between no dispersion and calibrated dispersion, under three counterfactual scenarios that each shut down one mechanism at a time. “No Amenity Externality” removes the effect of pollution on local amenities; “No Productivity Externality” removes its impact on firm productivity; “No Migration” fixes population distributions across provinces. The baseline welfare cost with all channels active is 1%. Comparing each bar to the baseline isolates the contribution of the shut-down channel.

To further explore how welfare varies with dispersion intensity, we run a sequence of counterfactual economies in which we progressively scale the bilateral pollutant-flow matrix from purely local dispersion to the baseline level of cross-border transport. This delivers the aggregate and provincial lifetime-welfare effects as a function of dispersion intensity. Specifically, we parameterise the varying bilateral pollutant-flow matrix as

$$\Phi(\theta) \equiv \theta \rho + (1 - \theta) I, \quad \theta \in [0, 1],$$

where ρ is the calibrated trajectory-based bilateral pollutant-flow matrix, I is the identity matrix. By construction, $\Phi(\theta)$ is a linear combination of the calibrated trajectory-based bilateral pollutant-flow matrix and identity matrix, so total emissions are conserved while we vary how much stays local vs. travels.

Figure 10 and Table A7 reports consumption-equivalent welfare across Chinese provinces under a transition from full localization ($\theta = 0$) to the empirically calibrated level of cross-provincial dispersion ($\theta = 1$), holding fixed economic fundamentals. At the aggregate level, welfare falls

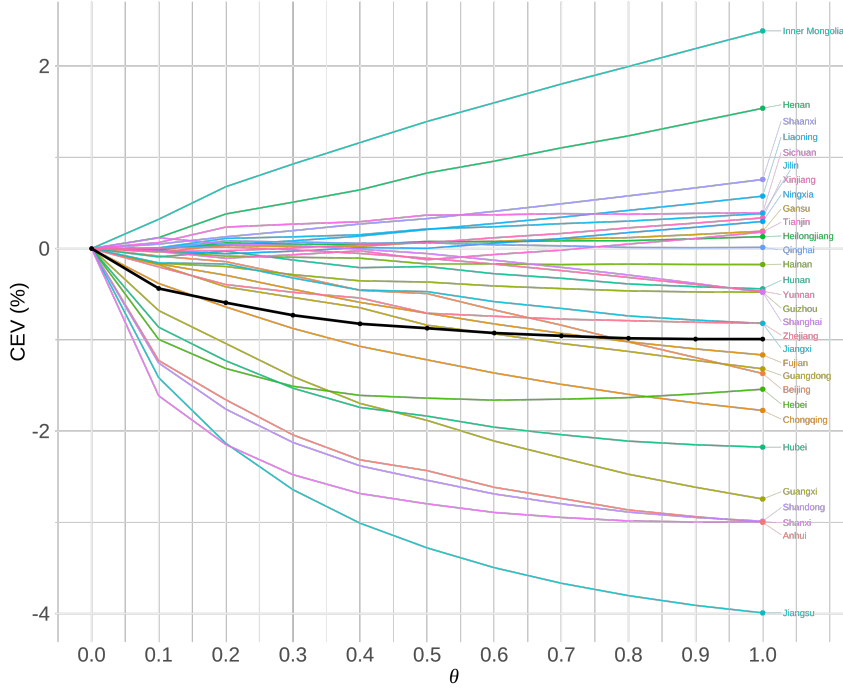
as transboundary dispersion is introduced. As θ increases towards 1, aggregate welfare declines almost monotonically, ending roughly 1% below the fully local benchmark. The mechanism is straightforward: when pollution can travel, exposure spreads to a larger population and this raises the national welfare cost even if some regions gain. It is worth to note that while aggregate welfare declines as θ rises, the relationship flattens rapidly. However, the distributional implications differ sharply: As more and more transboundary air pollution moves across regions, it amplifies the welfare gains and losses.

Two mechanisms could explain this divergence between aggregate and distributional effects. First, the extensive margin dominates at low dispersion levels. When θ is small, atmospheric transport begins to carry pollution from inland to the densely populated eastern provinces where the marginal damage from pollution is high. This generates large aggregate welfare losses as populations become more exposed. At higher θ , downwind provinces already bear substantial transboundary burdens. Further increases in dispersion primarily reshuffle pollution among provinces already experiencing elevated concentrations. A reallocation along the intensive margin generates smaller changes in aggregate exposure.

Second, concavity in pollution damages dampens aggregate effects while preserving distributional impacts. Our calibrated amenity function exhibits decreasing marginal disutility of pollution: an additional unit of PM_{2.5} causes less harm in provinces already experiencing high concentrations. When transport reallocates pollution from a high-concentration upwind province to a moderate-concentration downwind province, the amenity loss at the destination is smaller than the amenity gain at the source, reducing net aggregate damages. Yet the distributional consequences remain large: the same reallocation creates clear winners and losers across provinces, even if national welfare changes modestly. Together, these forces stabilize aggregate welfare while allowing substantial redistribution of pollution burdens across space.

These results have direct implications for policy design. The near-flat aggregate welfare curve at high dispersion levels suggests that mismeasuring the transport matrix—a common concern given the complexity of atmospheric modeling—may have limited aggregate welfare consequences. A policymaker who underestimates θ by 20% would incur only a 0.2-0.3 percentage point error in national welfare calculations. However, the distributional implications are first-order: the same 20% error would misallocate pollution burdens across provinces by several percentage points of welfare, misidentifying winners and losers and potentially undermining political feasibility of reforms. This asymmetry motivates our focus in Section 7 on policies that explicitly account for spatial externalities, allocating abatement responsibility based on estimated transport relationships rather than treating all provinces symmetrically.

Figure 10: Welfare impact with respect to dispersion intensity



Notes: The figure plots province-level consumption-equivalent welfare (CEV, %) as we move from fully local emissions ($\theta=0$) to the calibrated transboundary dispersion ($\theta=1$). Fundamentals and the calibrated policy path are held fixed; for each θ the spatial equilibrium is resolved, and CEV is measured relative to $\theta=0$ with 2002 labor weights. The black line represents the national aggregate welfare.

6.2 The Spatial Incidence of Local Emission Taxes

How do local emission taxes transmit benefits and costs through space? When one province tightens its pollution regulation, the welfare effects extend far beyond its borders: atmospheric transport carries abatement benefits to downwind regions, while general equilibrium adjustments propagate price and wage effects through the production network. We quantify these spatial spillovers by calculating the marginal effect of each province's emission tax on national welfare.

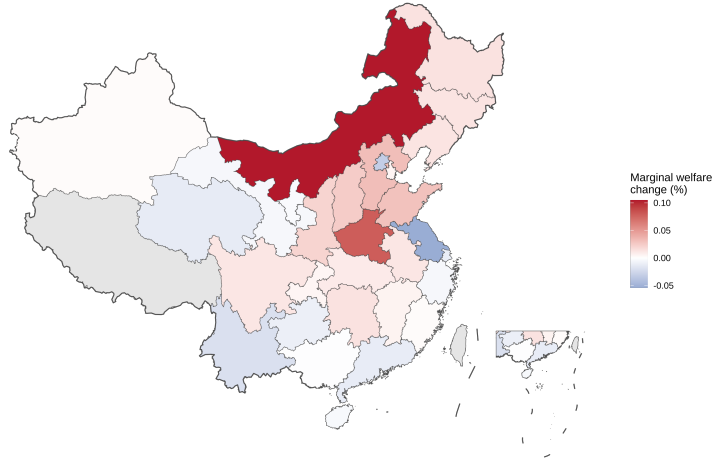
For each province m , we adjust its 2017 emission tax while keeping the taxes of all other provinces constant, and then resolve the dynamic spatial equilibrium model. The marginal national welfare effect is computed using a central difference approximation:

$$\frac{\Delta W}{\Delta \psi_m} \approx \sum_i w_i \times \frac{W_i(\psi_m + h) - W_i(\psi_m - h)}{2h},$$

where ψ_m is the emission tax rate of province m , $W_i(\psi_m)$ is the welfare of province i under tax ψ_m , $w_i = L_i^{2002} / \sum_j L_j^{2002}$ is the welfare weight with initial labour.² This gradient measures the social welfare of emission tax in province m , aggregating effects across all provinces and accounting for both atmospheric transport and economic adjustments.

²See more details in Appendix 5

Figure 11: Marginal national welfare effect of emissions-tax



Notes: The map reports the marginal welfare change from a one percentage point increase in each province’s emission tax, holding other provincial taxes constant. Red shading indicates regions where higher local taxation raises aggregate national welfare. Blue shading indicates provinces where additional taxation reduces aggregate welfare. The gradient highlights the spatial asymmetry in policy effectiveness—emission reductions in upwind, high-spillover provinces yield larger national welfare gains.

The spatial distribution of policy gradients is highly uneven. Figure 11 shows that a one percentage point increase in Inner Mongolia’s emission tax raises national welfare by 0.1%, the largest marginal effect in China. Other upwind northern and northwestern provinces—Henan, Shaanxi, Hebei—also exhibit large positive gradients. In contrast, most coastal and southeastern manufacturing provinces display marginal effects near zero or slightly negative.

What explains this spatial heterogeneity in welfare gradients? When a province tightens its emission tax, four forces shape the national welfare effect. First, higher production costs reduce output locally, lowering consumption and raising prices. This negative effect can be amplified through production networks. Second, reduced emissions improve local amenity as air quality improves. Third, reduced emissions raise local productivity as pollution’s drag on output diminishes. Fourth, reduced emissions improve amenity and productivity in downwind provinces through lower transboundary pollution. The net welfare gradient reflects the balance of these forces.

Upwind provinces with large spillovers exhibit the highest gradients. When Inner Mongolia tightens its tax, the direct production cost is local, but amenity and productivity benefits accrue to populous downwind regions. Coastal provinces exhibit small or negative gradients despite severe local pollution. A number of these provinces are crucial suppliers of intermediate goods. For instance, Jiangsu’s manufacturing industry feeds into nationwide production networks. Consequently, higher costs there spread widely through input-output linkages. The ultimate effect is a reduction in overall consumption. Lower emissions improve local amenities and productivity. Given these provinces are downwind, these positive spillover effects are limited in other provinces. The net effect turns negative: tightening taxes imposes first-order production costs while delivering only

modest additional environmental benefits.

These patterns are consistent with the geography of pollutant dispersion and the structure of interregional linkages. Upwind provinces with substantial outflows to populous downwind areas generate large national benefits when their pollution is regulated: a small local tax increase reduces exposure for many external residents thus reducing its negative externality on other provinces. In contrast, provinces that retain a large share of their own emissions gain little from additional local tightening; in those locations, general-equilibrium mechanism through prices can offset environmental benefits, yielding gradients close to zero or negative values.

This spatial heterogeneity carries a direct implication: provinces differ dramatically in their marginal contribution to national welfare. Inner Mongolia generates 0.105% welfare gain from a one percentage point tax increase, while Jiangsu generates -0.054%—a 0.16 percentage point difference. This gap reflects where abatement delivers the greatest social returns. Tightening emission taxes in upwind provinces like Inner Mongolia and Henan—where pollution travels to densely populated downwind regions—produces outsized national benefits. Conversely, further tightening in coastal provinces whose emissions remain local yields minimal additional gains and may even reduce national welfare through the negative effect on production. These gradients suggest substantial efficiency improvements from reallocating abatement effort to match the spatial structure of atmospheric transport and economic activity. We investigate this reallocation in the next section.

7 Welfare Effects of Alternative Allocation Rules

How should China allocate pollutant reduction responsibility across provinces? Our analysis reveals substantial spatial externalities: provinces differ dramatically in how much pollution they export, where it travels, and whom it harms. We evaluate the welfare impact of China’s 2013 Air Pollution Prevention and Control Action Plan, then compare it to alternative allocation rules. All allocations target the same aggregate reduction, allowing us to isolate the welfare consequences of how reduction burdens are distributed across space.

7.1 China’s Air Pollution Prevention and Control Action Plan

China’s 2013 Air Pollution Prevention and Control Action Plan (APPCAP) marked the nation’s first official policy mandating reductions in ambient PM_{2.5} concentrations. The plan established differentiated reduction targets for three key economic regions, mandating cuts in PM_{2.5} concentration by 2017 relative to 2013 levels. The required reductions were set at 25% for the Beijing-Tianjin-Hebei (BTH) region, 20% for the Yangtze River Delta (YRD), and 15% for the Pearl River Delta (PRD). The policy followed a top-down implementation structure. The central government sets the aggregate regional targets and provides general guidance, while delegating the authority and responsibility for implementation to provincial governments. Under this framework, provinces developed their own policy mixes to comply with the mandates. Crucially, pollution reduction performance

was formally incorporated into the evaluation system for provincial officials, creating a powerful career incentive for local leaders to achieve the targets. The derivation of these specific numerical targets was not explicitly detailed in the policy documents. However, the APPCAP was formulated in direct response to the severe air quality crises and widespread public concerns during 2010-2012. In this context, the most polluted, politically salient, and densely populated megacities naturally became the focal point of national mitigation efforts.

To evaluate the welfare impact of APPCAP, we simulate the policy in our calibrated model using an ex-ante approach that uses information available to policymakers in 2012. The logic proceeds as follows. In the baseline 2012 economy, the central government launches APPCAP by assigning reduction targets to each province. Provincial governments, observing the same economic conditions, implement policies to achieve their assigned targets. In the model, policy stringency is captured by the emission tax rate. We use the model's first-order conditions to back out the province-specific tax rate that would induce firms to achieve APPCAP's targeted emission levels.

Formally, denote the three priority regions as \mathcal{R}_1 (BTH), \mathcal{R}_2 (YRD), and \mathcal{R}_3 (PRD), with reduction rates $r_1 = 0.25$, $r_2 = 0.20$, and $r_3 = 0.15$. The allocation is:

$$e_{2017}^{n,*} = e_{2012}^n - E_{2012}^n \times r_k \text{ if } n \in \mathcal{R}_k, k \in \{1, 2, 3\},$$

where E_{2012}^n is the pollution stock at baseline 2012 economy, e_{2012}^n is the emission level, $e_{2012}^{n,*}$ is the targeted emission level in 2017 under the APPCAP. Therefore, the emission tax that rationalizes this target, derived from the firm's first-order condition, is

$$\psi_{2017}^{n,*} = \frac{VA_{2012}^n}{e_{2017}^{n,*}}$$

where VA_{2012}^n is the value added in province n in the baseline economy. This counterfactual tax represents the shadow price of the emission constraint implied by APPCAP's allocation.

We solve for the sequential equilibrium under these province-specific emission taxes following the procedure described above. We evaluate APPCAP against a counterfactual that holds all emission taxes fixed at their 2012 levels, i.e. no new post-2012 controls. Relative to the counterfactual, we find that APPCAP increases national welfare by 0.2%.

This magnitude reflects a balance of offsetting forces embedded in the model. On the benefit side, sharp reductions in $PM_{2.5}$ within BTH, YRD, and PRD deliver large amenity gains and modest productivity improvement. These gains are tempered by general-equilibrium costs: emission taxes raise abatement effort and unit costs, which pass through to the consumption price index, eroding part of the improvement in real income; transboundary inflows from upwind regions limit how much local ambient air can improve even when local emissions fall; and interprovincial migration frictions keep the spatial reallocation response small, so high-gain locations cannot fully capitalize on improved conditions by drawing in population. Finally, because APPCAP allocates cuts by where pollution is concentrated rather than by where a marginal cut yields the largest national benefit, it limits the ability that policy can achieve higher aggregate welfare gains.

7.2 Alternative Emission Allocation Rules

This section we now ask whether alternative allocation rules could achieve higher welfare while meeting the same aggregate reduction target. We compare APPCAP to three counterfactual allocations that differ in how they distribute reduction burdens across provinces. This comparison isolates the welfare consequences of spatial allocation design, holding fixed the total pollution reduction and the economic information available in the baseline period.

All four allocation rules follow a common implementation procedure. We first define the aggregate reduction target M based on APPCAP's allocation. Applying APPCAP's regional mandates to baseline 2012 pollution yields:

$$M = 0.25 \sum_{n \in \text{BTH}} E_{2012}^n + 0.20 \sum_{n \in \text{YRD}} E_{2012}^n + 0.15 \sum_{n \in \text{PRD}} E_{2012}^n, \quad (19)$$

which measures the total pollution reduction targeted under APPCAP. Each of the four allocation rules distributes this same aggregate target M across provinces according to different principles. For a given allocation rule, let $e_{2017}^{n,*}$ denote the targeted 2017 emission level assigned to province n . The allocation must satisfy the aggregate constraint:

$$\sum_n (e_{2012}^n - e_{2017}^{n,*}) = M. \quad (20)$$

This constraint ensures that all four rules target identical aggregate pollution reduction, differing only in how they distribute the reduction burden spatially.

To implement these targets in the model, we back out the emission tax rate required in each province to achieve its target, as described in the previous section. We then solve for the sequential equilibrium under these province-specific tax schedules.

The three alternative allocation rules are as follows.

Rule 1: Uniform Reduction

The simplest allocation assigns equal absolute emission cuts to all provinces, regardless of baseline emissions or spillover patterns:

$$e_{2017}^{n,*} = e_{2012}^n - \frac{M}{N},$$

where N is the number of provinces, e_{2012}^n is the emission level in baseline economy 2012, $e_{2017}^{n,*}$ is the targeted emission level in 2017 under the allocation rule. Each province reduces emissions by M/N tons. This rule resembles an equal-quota scheme-straightforward to implement, transparent, and perhaps appealing on equity grounds. However, it ignores both economic efficiency and environmental effectiveness. A ton of abatement in Inner Mongolia has very different social value than a ton in Guangdong, yet this rule treats them identically.

Rule 2: Proportional to Baseline Emissions

A natural refinement allocates reduction targets proportionally to each province's baseline emissions, implementing a “more emissions, more abatement” principle:

$$e_{2017}^{n,*} = e_{2012}^n - \frac{e_{2012}^n}{\sum_k e_{2012}^k} \times M.$$

Provinces that emit more in 2012 bear larger absolute cuts. This rule embodies a polluter-pays philosophy and preserves cross-province proportionality. However, like Rule 1, it ignores where pollution travels. A high-emitting province whose pollution blows out to less populous regions is treated the same as an equally high-emitting province whose pollution reaches mega cities—a clear inefficiency when transboundary flows vary dramatically. This approach ends up each province faces the same percentage reduction.

Rule 3: Marginal-welfare-weighted Policy

An optimal policy of emission tax rate would solve for the full vector of provincial emission taxes that maximizes national welfare subject to constraints, equalizing marginal social welfare per unit abatement across locations. Because that high-dimensional, dynamic problem is computationally onerous, we do not attempt to solve it globally. Instead, we calculated policy gradients in Section 6.2, the partial derivatives of national welfare with respect to each province’s emissions tax. We use these marginal welfare to design allocation rules that direct greater effort toward provinces with higher gradients. While this rule is not able to characterize the global optimum, it delivers first-order improvements around the baseline. This strategy is transparent, aligns with the underlying economic model, and provides a way to address cross-regional pollution effects—moving the system closer to the ideal of equal marginal social benefits across provinces.

In Section 6.2, we measure the marginal national welfare gain for each provincial emission tax, denoted as g_n . The allocation weights are then taken to be the positive part of these gradients:

$$w_n \equiv \max \{g_n, 0\}, \quad \tilde{w}_n = \frac{w_n}{\sum_k w_k}$$

Intuitively, \tilde{w}_n is proportional to the marginal social value of tightening in province n . Provinces where a marginal tax increase raises national welfare more receive a larger share of the national abatement mandate. Therefore, the province-level target is

$$e_{2017}^{n,*} = e_{2012}^n - \tilde{w}_n M$$

This rule is Pigouvian in the sense that it allocates abatement where the model indicates the highest marginal national benefit, internalizing upwind-downwind spillovers. Provinces with negative gradients ($g_n < 0$) receive zero weight under this rule reflecting that, at the baseline policy, a further local tightening would reduce national welfare.

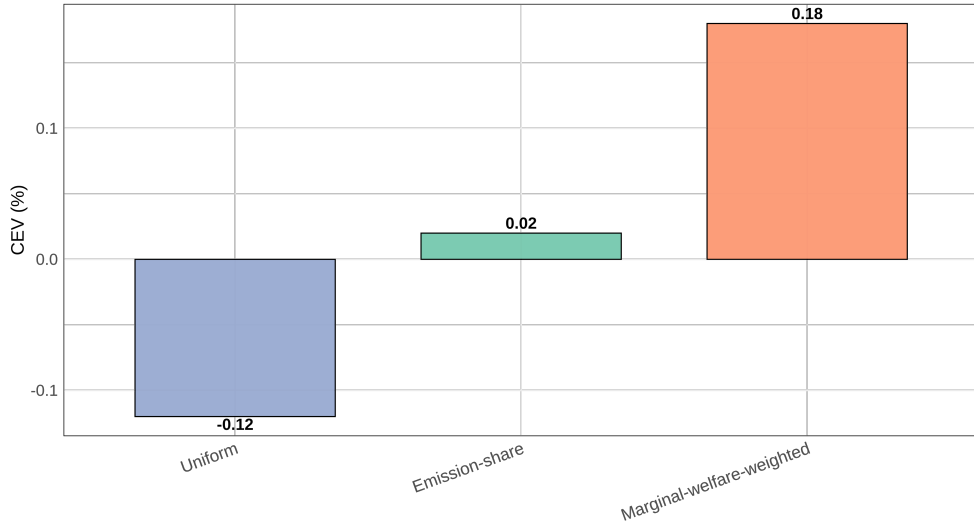
7.3 The Geography of Pollutant Control and Welfare Impact

How do alternative allocation rules shape the geography of pollutant control and welfare outcomes? We compare four approaches that differ fundamentally in their allocation principles.

The spatial distribution of abatement burdens varies dramatically as shown in Figure A4. Under a uniform allocation scheme, reduction burden is heavier for cleaner regions: Hainan, an isolated island province reliant on tourism, faces the largest cut of 29%, whereas Hebei, dominated by heavy raw-material industries, faces only a 3% reduction. Proportional allocation spreads a uniform 6% reduction rate across all provinces. The APPCAP concentrates regulatory effort where local pollution is most severe and politically salient. Yet neither proportional nor APPCAP accounts for transboundary flows. The marginal-welfare-weighted rule produces the steepest spatial pattern. Abatement concentrates sharply in the northern corridor, while coastal manufacturing provinces see smaller reduction burden relative to its emission level. This reflects a fundamentally different allocation logic: regions where abatement generates higher social returns through its effects on the spatial economy bear higher burden.

These spatial patterns translate directly into welfare outcomes shown in Figure 12. Uniform allocation's perverse distribution produces the worst result: 0.12% welfare loss relative to APPCAP. By imposing heavy cuts on low-emission provinces with limited industrial capacity, it achieves reduction where most costly and least effective. Proportional allocation improves modestly by +0.02% compared to APPCAP. Yet substantial welfare improvements remain available. The marginal-welfare-weighted rule delivers 0.18% welfare gain relative to APPCAP by systematically exploiting spatial externalities. This allocation targets provinces not because their local air quality is poor, but because their emissions cut can generate larger national welfare gains through the spatial economy.

Figure 12: Aggregate Welfare under Alternative Allocation Rules



Notes: Bars report national consumption-equivalent variation (CEV, %) for different allocation rules relative to the baseline case which reflects Chinese Air Pollution Prevention and Control Action Plan. Positive values indicate higher national welfare relative to the baseline.

8 Conclusion

This paper brings together new evidence on spatial spillover of air pollution and a dynamic spatial general equilibrium model to quantify how transboundary air pollution reshapes welfare and to evaluate policy design when pollution crosses borders. We construct bilateral PM_{2.5} transport matrices using particle trajectory data from atmospheric models, revealing three empirical patterns. Trans-boundary exposure is highly heterogeneous-ranging from negligible in isolated inland provinces to over 50% in coastal manufacturing regions. Transport networks exhibit temporal stability, governed by persistent wind corridors rather than transient weather. And economically advanced provinces receive disproportionate transboundary inflows, creating a geographic mismatch between emission sources and damage locations.

Embedding the estimated pollutant-flow matrix into a multi-region, multi-sector spatial model with migration and trade, we isolate the contribution of pollution dispersion to welfare. Relative to a benchmark with fully localized emissions, allowing cross-boundary transport lowers national welfare by about 1% while generating large distributional impacts. As dispersion intensifies, the aggregate loss rises but quickly flattens, whereas effects for each province diverge: upwind and inland provinces often gain as some of their emissions are exported, while eastern manufacturing hubs lose as they import more pollution.

We evaluate China’s 2013 Air Pollution Prevention and Control Action Plan, which concentrated reduction targets in three polluted regions (Beijing-Tianjin-Hebei, Yangtze Delta, Pearl Delta) but ignored transboundary flows in its design. Comparing APPCAP to alternative allocation rules, we find that reallocating abatement to high-spillover upwind provinces based on each province’s marginal social value of emission tax improves aggregate welfare by 0.18% relative to APPCAP. Therefore, China’s actual policy achieves middle-ground efficiency, capturing some gains from spatial differentiation despite not explicitly modeling atmospheric transport. However, substantial welfare improvements remain available from incorporating transboundary flows into allocation design.

Future work should incorporate endogenous abatement investment and fiscal transfers, as well as explore algorithms to solve the full optimal spatial tax problem. Nonetheless, the central message remains clear: when pollution ignores borders, policy must not. By calibrating to the physical flow of pollutants and targeting marginal social benefits, national welfare can be improved.

References

- Ambec, Stefan, Federico Esposito, and Antonia Pacelli.** 2024. “The economics of carbon leakage mitigation policies.” *Journal of Environmental Economics and Management*, 125: 102973.
- Arceo, Eva, Rema Hanna, and Paulina Oliva.** 2016. “Does the effect of pollution on infant mortality differ between developing and developed countries? Evidence from Mexico City.” *The Economic Journal*, 126(591): 257–280.
- Balboni, Clare.** 2025. “In harm’s way? infrastructure investments and the persistence of coastal cities.” *American Economic Review*, 115(1): 77–116.
- Balboni, Clare A, and Joseph S Shapiro.** 2025. “Spatial Environmental Economics.” National Bureau of Economic Research.
- Bilal, Adrien, and Diego R Käenzig.** 2024. “The macroeconomic impact of climate change: Global vs. local temperature.” National Bureau of Economic Research.
- Borgschulte, Mark, David Molitor, and Eric Yongchen Zou.** 2024. “Air pollution and the labor market: Evidence from wildfire smoke.” *Review of Economics and Statistics*, 106(6): 1558–1575.
- Caliendo, Lorenzo, and Fernando Parro.** 2015. “Estimates of the Trade and Welfare Effects of NAFTA.” *The Review of Economic Studies*, 82(1): 1–44.
- Caliendo, Lorenzo, and Fernando Parro.** 2022. “Trade policy.” *Handbook of international economics*, 5: 219–295.
- Caliendo, Lorenzo, Maximiliano Dvorkin, and Fernando Parro.** 2019. “Trade and labor market dynamics: General equilibrium analysis of the china trade shock.” *Econometrica*, 87(3): 741–835.
- Chan, H Ron, B Andrew Chupp, Maureen L Cropper, and Nicholas Z Muller.** 2018. “The impact of trading on the costs and benefits of the Acid Rain Program.” *Journal of Environmental Economics and Management*, 88: 180–209.
- Chen, Shiyi, Joshua S Graff Zivin, Huanhuan Wang, and Jiaxin Xiong.** 2022. “Combating cross-border externalities.” National Bureau of Economic Research.
- Chen, Shuai, Paulina Oliva, and Peng Zhang.** 2022. “The effect of air pollution on migration: Evidence from China.” *Journal of Development Economics*, 156: 102833.
- Chen, Yvonne Jie, Pei Li, and Yi Lu.** 2018. “Career concerns and multitasking local bureaucrats: Evidence of a target-based performance evaluation system in China.” *Journal of Development Economics*, 133: 84–101.
- CLRTAP.** 1979. “Development of the Convention on Long-range Transboundary Air Pollution.”

- Coase, Ronald H.** 1960. “The Problem of Social Cost.” *Journal of Law and Economics*, 3: 1–44.
- Crippa, Monica, Efisio Solazzo, Ganlin Huang, Diego Guizzardi, Ernest Koffi, Marilena Muntean, Christian Schieberle, Rainer Friedrich, and Greet Janssens-Maenhout.** 2020. “High resolution temporal profiles in the Emissions Database for Global Atmospheric Research.” *Scientific data*, 7(1): 121.
- Cruz, José-Luis, and Esteban Rossi-Hansberg.** 2024. “The economic geography of global warming.” *Review of Economic Studies*, 91(2): 899–939.
- Deryugina, Tatyana, Garth Heutel, Nolan H Miller, David Molitor, and Julian Reif.** 2019. “The mortality and medical costs of air pollution: Evidence from changes in wind direction.” *American Economic Review*, 109(12): 4178–4219.
- Desmet, Klaus, Dávid Krisztián Nagy, and Esteban Rossi-Hansberg.** 2018. “The geography of development.” *Journal of Political Economy*, 126(3): 903–983.
- Domínguez-Iino, Tomás.** 2023. “Spatial economics and environmental policies.” *Handbook of Labor, Human Resources and Population Economics*, 1–16.
- Eaton, Jonathan, and Samuel Kortum.** 2002. “Technology, geography, and trade.” *Econometrica*, 70(5): 1741–1779.
- Ebenstein, Avraham, Maoyong Fan, Michael Greenstone, Guojun He, Peng Yin, and Maigeng Zhou.** 2015. “Growth, pollution, and life expectancy: China from 1991–2012.” *American Economic Review*, 105(5): 226–231.
- Fowlie, Meredith, and Nicholas Muller.** 2013. “Market-based emissions regulation when damages vary across sources: What are the gains from differentiation?” National Bureau of Economic Research.
- Fu, Shihe, V Brian Viard, and Peng Zhang.** 2021. “Air pollution and manufacturing firm productivity: Nationwide estimates for China.” *The Economic Journal*, 131(640): 3241–3273.
- Fu, Shihe, V Brian Viard, and Peng Zhang.** 2022. “Trans-boundary air pollution spillovers: Physical transport and economic costs by distance.” *Journal of Development Economics*, 155: 102808.
- GBD.** 2020. “Global burden of 87 risk factors in 204 countries and territories, 1990–2019: a systematic analysis for the Global Burden of Disease Study 2019.” *The Lancet*, 396(10258): 1223–1249.
- Greenstone, Michael, Christa Hasenkopf, and Ken Lee.** 2022. “Air Quality Life Index: Annual Update 2022.” Energy Policy Institute at the University of Chicago (EPIC).
- Hanna, Rema, and Paulina Oliva.** 2015. “The effect of pollution on labor supply: Evidence from a natural experiment in Mexico City.” *Journal of Public Economics*, 122: 68–79.

- Heblich, Stephan, Alex Trew, and Yanos Zylberberg.** 2021. “East-side story: Historical pollution and persistent neighborhood sorting.” *Journal of Political Economy*, 129(5): 1508–1552.
- HEI.** 2022. “State of Global Air 2022: A special report on global exposure to air pollution and its health impacts.” Health Effects Institute, Boston, MA.
- Henderson, J Vernon.** 2007. “Understanding knowledge spillovers.” *Regional Science and Urban Economics*, 37(4): 497–508.
- Heo, Seonmin Will, Koichiro Ito, and Rao Kotamarthi.** 2023. “International spillover effects of air pollution: evidence from mortality and health data.” National Bureau of Economic Research.
- Khanna, Gaurav, Wenquan Liang, Ahmed Mushfiq Mobarak, and Ran Song.** 2021. “The productivity consequences of pollution-induced migration in China.” National Bureau of Economic Research.
- Lin, Jintai, Da Pan, Steven J Davis, Qiang Zhang, Kebin He, Can Wang, David G Streets, Donald J Wuebbles, and Dabo Guan.** 2014. “China’s international trade and air pollution in the United States.” *Proceedings of the National Academy of Sciences*, 111(5): 1736–1741.
- Montgomery, W David.** 1972. “Markets in licenses and efficient pollution control programs.” *Journal of economic theory*, 5(3): 395–418.
- Pigou, Arthur Cecil.** 1920. *The Economics of Welfare*. London:Macmillan.
- Pleim, Jonathan E, Limei Ran, Rick D Saylor, Jeff Willison, and Francis S Binkowski.** 2022. “A new aerosol dry deposition model for air quality and climate modeling.” *Journal of advances in modeling earth systems*, 14(11): e2022MS003050.
- Shapiro, Joseph S, and Reed Walker.** 2018. “Why is pollution from US manufacturing declining? The roles of environmental regulation, productivity, and trade.” *American economic review*, 108(12): 3814–3854.
- Taylor, M Scott, and Brian R Copeland.** 2003. *Trade, growth and the environment*. Citeseer.
- Tombe, Trevor, and Xiaodong Zhu.** 2019. “Trade, migration, and productivity: A quantitative analysis of China.” *American Economic Review*, 109(5): 1843–1872.
- Van Donkelaar, Aaron, Melanie S Hammer, Liam Bindle, Michael Brauer, Jeffery R Brook, Michael J Garay, N Christina Hsu, Olga V Kalashnikova, Ralph A Kahn, Colin Lee, et al.** 2021. “Monthly global estimates of fine particulate matter and their uncertainty.” *Environmental Science & Technology*, 55(22): 15287–15300.
- Wang, Mengyuan, Zi Wang, and Zhengying Xie.** 2024. “Optimal Spatial Emission.” *Working paper*.

Wang, Xiaoxi, Meng Xu, and Kevin Chen. 2025. “Internalizing Externalities through Ecological Compensation: Evidence from Transboundary Water Pollution in China.” *Journal of Environmental Economics and Management*, 103200.

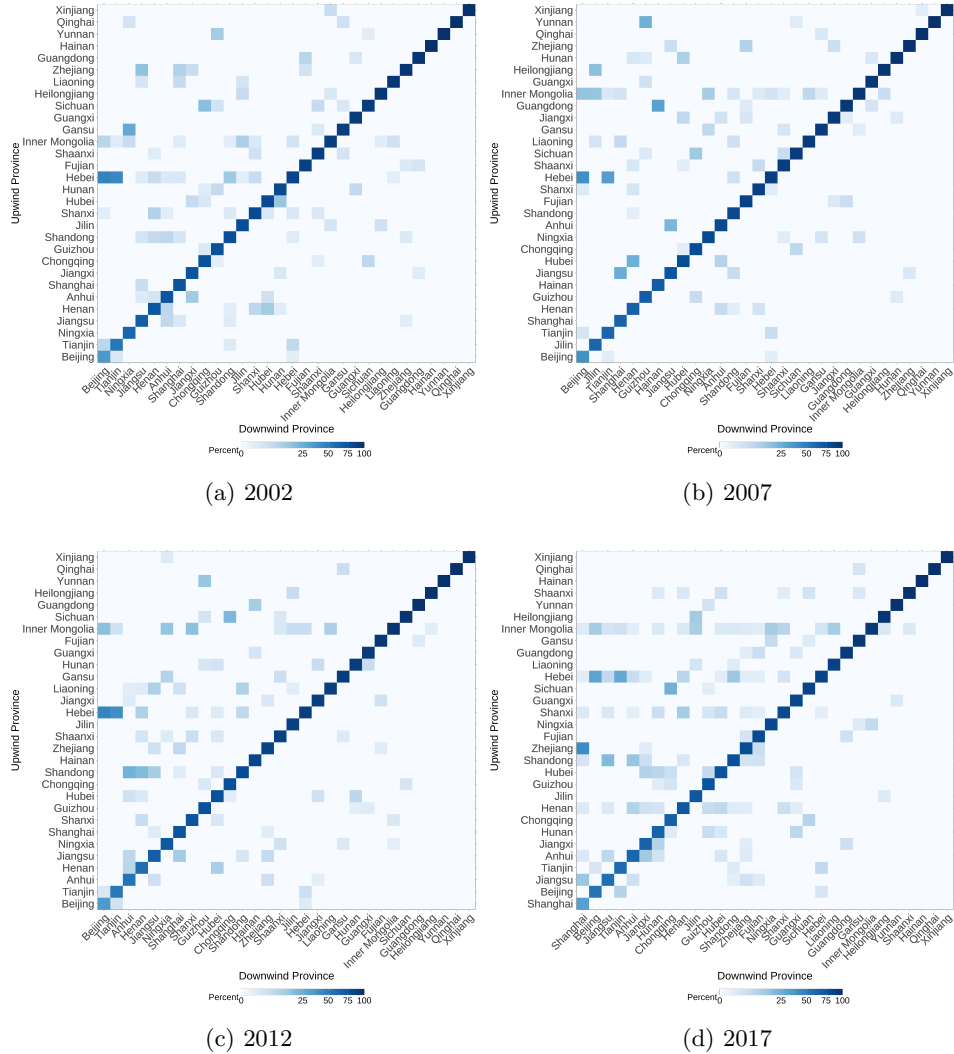
Zhang, Yuqiang, Rohit Mathur, Jesse O Bash, Christian Hogrefe, Jia Xing, and Shawn J Roselle. 2018. “Long-term trends in total inorganic nitrogen and sulfur deposition in the US from 1990 to 2010.” *Atmospheric chemistry and physics*, 18(12): 9091–9106.

Zhao, Qiong, Chen Pan, Zengkai Zhang, Xuefan Guo, Kunfu Zhu, Jianwu He, and Shantong Li. 2024. “An inter-regional input-output table series of China from 1987–2017 with integrated carbon emission data.” *Scientific Data*, 11(1): 1335.

Zivin, Joshua Graff, and Matthew Neidell. 2012. “The impact of pollution on worker productivity.” *American Economic Review*, 102(7): 3652–3673.

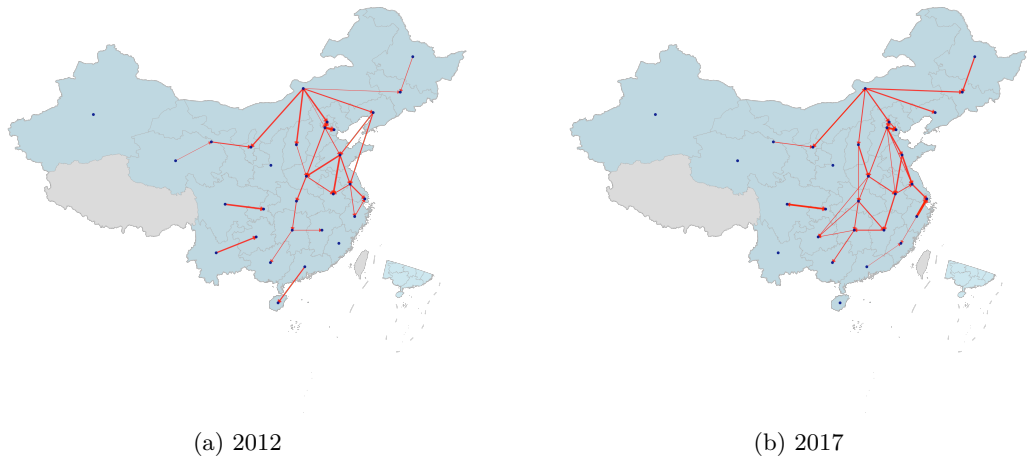
Appendix

1 Figures and Tables



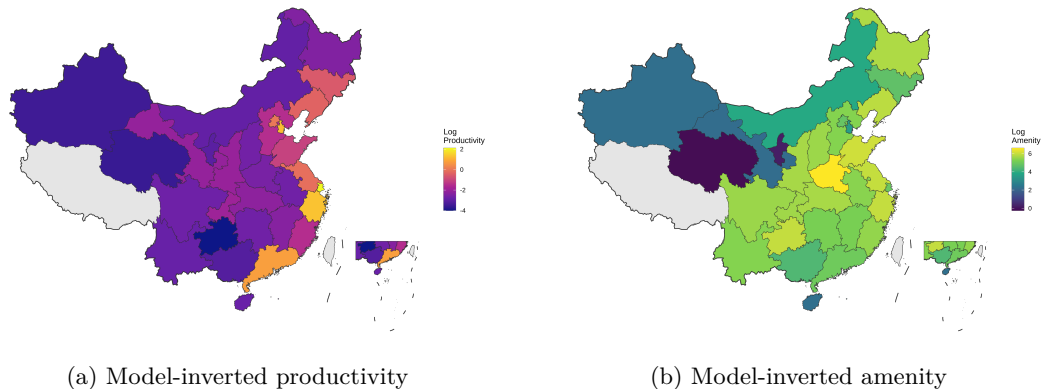
Appendix Figure A1: Bilateral pollutant-flow Matrix

Notes: This figure plots the bilateral pollutant-flow matrix across Chinese provinces for the years 2002, 2007, 2012, and 2017. The rows represent the source provinces and the columns represent the receptor provinces. The diagonal cells measure the share of locally generated pollution that remains within the same province, while the off-diagonal cells capture cross-province transmission. Darker colors indicate a higher contribution share. The comparison across years highlights the evolution of pollutant transmission patterns over time, with both the magnitude of transboundary flows and the heterogeneity across provinces becoming more evident in later years.



Appendix Figure A2: Major Pollutant-flow Network ($>5\%$)

Notes: The maps show the major pollutant-flow network in 2012 and 2017. Red arrows show “major” cross-provincial pollution links—pairs for which the bilateral flow share exceeds 5%. The backbone runs from inland/northern sources toward the Beijing–Tianjin–Hebei region and the Yangtze River Delta.



Appendix Figure A3: Model-inverted fundamentals

Notes: This figure displays the spatial distribution of model-inverted fundamentals in the baseline year 2002. Panel (a) shows the model-inverted average productivity, capturing regional differences in production efficiency implied by equilibrium outcomes. Panel (b) shows the model-inverted amenity, implied from local wages, prices, and migration decisions.

Appendix Table A1: First stage of the Impact of PM_{2.5} on Productivity and Amenity

	First stage
Dependent variable: log PM _{2.5}	
Log(strength in thermal inversion)	0.11 (0.05)
Province FE	✓
Year FE	✓
Observations	90
KP F-statistics	10.86

Notes: We have three periods in our study: 2002-2006, 2007-2011, 2012-2017. The dependent variable is PM_{2.5} concentration, which also measures the five-year average. Thermal inversion strength is defined using above-ground temperature minus ground temperature. A positive difference indicates the existence of a thermal inversion and the magnitude measures the inversion strength. We also measure it at five-year interval. Controls include GDP, precipitation, wind speed and humidity. Standard errors are listed in parentheses.

Appendix Table A2: IV Estimates of the Impact of PM_{2.5} on Productivity and Amenity

	(1)	(2)	(3)	(4)
	Agri prod.	Manuf prod.	Ser prod.	Amenity
2SLS				
Dependent variable: Log Productivity/Amenity				
log PM _{2.5}	-0.10 (0.06)	-0.06 (0.04)	-0.04 (0.03)	-0.18 (0.09)
GDP	✓	✓	✓	✓
Precipitation	✓	✓	✓	✓
Province FE	✓	✓	✓	✓
Year FE	✓	✓	✓	✓
Observations	90	90	90	90
R ²	0.98	0.99	0.99	0.18

Notes: Panel A estimates sectoral productivity damages using $\log A_{it}^j = \delta_i^j + \eta_a^j \log(\text{con}_{it}) + \text{FE} + \varepsilon_{it}^j$, where i indexes provinces, j sectors, t years, and E_{it} is local PM_{2.5}. Specifications include province and year fixed effects. Productivity is inverted from the model for each province-sector for year 2002, 2007, 2012 and 2017. Panel B estimates amenity damages using $\log B_{it} = \gamma_i + \eta_b \log(\text{con}_{it}) + \text{FE} + u_{it}$ with province and year fixed effects. Amenity is inverted from the model for each region for year 2002, 2007 and 2012. Standard errors are in the parenthesis.

Appendix Table A3: PM_{2.5} Passthrough Coefficients — 2002–2006

Upwind Hours	Without controls	With controls
$h = 1$	0.197*** (0.039)	0.206*** (0.036)
$h = 2$	0.193*** (0.037)	0.200*** (0.034)
$h = 3$	0.199*** (0.044)	0.204*** (0.042)
$h = 4$	0.201*** (0.051)	0.205*** (0.051)
$h = 5$	0.192*** (0.056)	0.195*** (0.056)
$h = 6$	0.182*** (0.063)	0.182*** (0.064)
$h = 7$	0.182** (0.067)	0.179** (0.067)
$h = 8$	0.173** (0.071)	0.169** (0.072)
$h = 9$	0.147* (0.073)	0.140* (0.074)
$h = 10$	0.128* (0.072)	0.118 (0.073)
$h = 11$	0.136* (0.072)	0.125* (0.073)
$h = 12$	0.129* (0.072)	0.117 (0.073)
$h = 13$	0.100 (0.070)	0.087 (0.071)
$h = 14$	0.083 (0.068)	0.068 (0.069)
$h = 15$	0.098 (0.070)	0.082 (0.071)
$h = 16$	0.096 (0.071)	0.080 (0.071)
$h = 17$	0.067 (0.068)	0.049 (0.069)
$h = 18$	0.050 (0.065)	0.033 (0.065)
$h = 19$	0.066 (0.069)	0.047 (0.069)
$h = 20$	0.065 (0.070)	0.046 (0.070)
$h = 21$	0.036 (0.066)	0.016 (0.066)
$h = 22$	0.020 (0.062)	0.000 (0.061)
$h = 23$	0.033 (0.068)	0.012 (0.067)
$h = 24$	0.032 (0.070)	0.012 (0.069)
$h = 25$	0.008 (0.066)	-0.012 (0.065)
$h = 26$	-0.003 (0.061)	-0.022 (0.060)
$h = 27$	0.008 (0.067)	-0.013 (0.066)
$h = 28$	0.009 (0.070)	-0.012 (0.068)
Observations	24,142,854	24,142,854
R ²	0.701	0.703

Notes: This table reports the passthrough coefficients of upwind PM_{2.5} on downwind concentrations over a 7-day period, which is partitioned into 28 non-overlapping 6-hour intervals. The dependent variable is the PM_{2.5} concentration at the destination location. The independent variables are the PM_{2.5} concentration of locations along the trajectory that are h -hour upwind from destination. Column (1) presents baseline estimates without additional controls. Column (2) includes a full set of controls, which comprise precipitation, wind speed, pressure, temperature and humidity. Both regressions include grid point fixed effect and month-by-year fixed effect. Standard errors, clustered at the province level, are reported in parentheses. Statistical significance is indicated by * $p < 0.10$, ** $p < 0.05$, and *** $p < 0.01$.

Appendix Table A4: PM_{2.5} Passthrough Coefficients —2007–2011

Upwind Hours	Without controls	With controls
$h = 1$	0.221*** (0.045)	0.227*** (0.044)
$h = 2$	0.217*** (0.043)	0.222*** (0.042)
$h = 3$	0.226*** (0.051)	0.232*** (0.051)
$h = 4$	0.233*** (0.062)	0.239*** (0.063)
$h = 5$	0.222*** (0.073)	0.226*** (0.075)
$h = 6$	0.203** (0.086)	0.204** (0.090)
$h = 7$	0.207** (0.088)	0.206** (0.091)
$h = 8$	0.197** (0.093)	0.194* (0.098)
$h = 9$	0.160 (0.098)	0.154 (0.103)
$h = 10$	0.132 (0.098)	0.124 (0.103)
$h = 11$	0.148 (0.096)	0.139 (0.101)
$h = 12$	0.144 (0.097)	0.133 (0.101)
$h = 13$	0.110 (0.095)	0.098 (0.100)
$h = 14$	0.090 (0.093)	0.077 (0.096)
$h = 15$	0.112 (0.094)	0.098 (0.099)
$h = 16$	0.115 (0.096)	0.100 (0.100)
$h = 17$	0.082 (0.092)	0.067 (0.096)
$h = 18$	0.060 (0.087)	0.045 (0.090)
$h = 19$	0.080 (0.090)	0.064 (0.094)
$h = 20$	0.082 (0.092)	0.065 (0.096)
$h = 21$	0.053 (0.087)	0.036 (0.090)
$h = 22$	0.035 (0.081)	0.019 (0.084)
$h = 23$	0.055 (0.086)	0.037 (0.089)
$h = 24$	0.055 (0.087)	0.037 (0.090)
$h = 25$	0.029 (0.081)	0.012 (0.084)
$h = 26$	0.015 (0.076)	-0.001 (0.078)
$h = 27$	0.034 (0.081)	0.016 (0.084)
$h = 28$	0.035 (0.083)	0.017 (0.086)
Observations	24,141,500	24,141,500
R ²	0.738	0.739

Notes: This table reports the passthrough coefficients of upwind PM_{2.5} on downwind concentrations over a 7-day period, which is partitioned into 28 non-overlapping 6-hour intervals. The dependent variable is the PM_{2.5} concentration at the destination location. The independent variables are the PM_{2.5} concentration of locations along the trajectory that are h -hour upwind from destination. Column (1) presents baseline estimates without additional controls. Column (2) includes a full set of controls, which comprise precipitation, wind speed, pressure, temperature and humidity. Both regressions include grid point fixed effect and month-by-year fixed effect. Standard errors, clustered at the province level, are reported in parentheses. Statistical significance is indicated by * $p < 0.10$, ** $p < 0.05$, and *** $p < 0.01$.

Appendix Table A5: PM_{2.5} Passthrough Coefficients —2012–2016

Upwind Hours	Without controls	With controls
$h = 1$	0.249*** (0.047)	0.253*** (0.047)
$h = 2$	0.244*** (0.046)	0.248*** (0.045)
$h = 3$	0.252*** (0.053)	0.257*** (0.053)
$h = 4$	0.258*** (0.061)	0.264*** (0.062)
$h = 5$	0.250*** (0.069)	0.254*** (0.072)
$h = 6$	0.233*** (0.081)	0.234*** (0.084)
$h = 7$	0.243*** (0.078)	0.243*** (0.082)
$h = 8$	0.234*** (0.084)	0.232** (0.089)
$h = 9$	0.195** (0.093)	0.190* (0.098)
$h = 10$	0.166* (0.094)	0.159 (0.100)
$h = 11$	0.196** (0.086)	0.188** (0.092)
$h = 12$	0.187** (0.088)	0.178* (0.094)
$h = 13$	0.140 (0.091)	0.130 (0.096)
$h = 14$	0.114 (0.091)	0.103 (0.095)
$h = 15$	0.149* (0.087)	0.137 (0.092)
$h = 16$	0.143 (0.088)	0.130 (0.093)
$h = 17$	0.101 (0.090)	0.087 (0.095)
$h = 18$	0.078 (0.089)	0.065 (0.093)
$h = 19$	0.113 (0.090)	0.098 (0.094)
$h = 20$	0.111 (0.091)	0.096 (0.095)
$h = 21$	0.069 (0.090)	0.055 (0.094)
$h = 22$	0.047 (0.086)	0.033 (0.089)
$h = 23$	0.080 (0.091)	0.065 (0.094)
$h = 24$	0.079 (0.092)	0.064 (0.096)
$h = 25$	0.044 (0.089)	0.029 (0.092)
$h = 26$	0.025 (0.083)	0.012 (0.086)
$h = 27$	0.056 (0.090)	0.041 (0.093)
$h = 28$	0.057 (0.091)	0.042 (0.094)
Observations	24,141,261	24,141,261
R ²	0.722	0.792

Notes: This table reports the passthrough coefficients of upwind PM_{2.5} on downwind concentrations over a 7-day period, which is partitioned into 28 non-overlapping 6-hour intervals. The dependent variable is the PM_{2.5} concentration at the destination location. The independent variables are the PM_{2.5} concentration of locations along the trajectory that are h-hour upwind from destination. Column (1) presents baseline estimates without additional controls. Column (2) includes a full set of controls, which comprise precipitation, wind speed, pressure, temperature and humidity. Both regressions include grid point fixed effect and month-by-year fixed effect. Standard errors, clustered at the province level, are reported in parentheses. Statistical significance is indicated by * $p < 0.10$, ** $p < 0.05$, and *** $p < 0.01$.

Appendix Table A6: Calibration Values

Parameter	Notation	Moment	Data
Labour share	ξ^{nj}	Share of wage bill in value-added	Regional I-O table
Value-added share	γ^{nj}	Share of value-added in gross output	Regional I-O table
Intermediate input share	$\gamma^{nj,nk}$	Share of intermediate input in gross output	Regional I-O table
Emission elasticity	λ^j	Emission productivity	EDGAR, CSY
Emission tax	ψ^{nj}	Emission productivity	EDGAR, CSY
Trade elasticity	θ^j	Caliendo and Parro (2015)	Literature
Migration elasticity	$1/v$	Tombe and Zhu (2019)	Literature
Trade cost	$\kappa^{nj,ij}$	Trade share	Regional I-O table
Migration cost	$\mu^{n,i}$	Migration share	Population census
Damage coefficient	η_a^j, η_b	IV estimation	SatPM
Productivity	A_t^{nj}	value-added	CSY, I-O table
Amenity	B_t^n	Kleinman el at. (2023)	Population census
Deposition rate	δ	PM _{2.5} concentration	SatPM + EDGAR

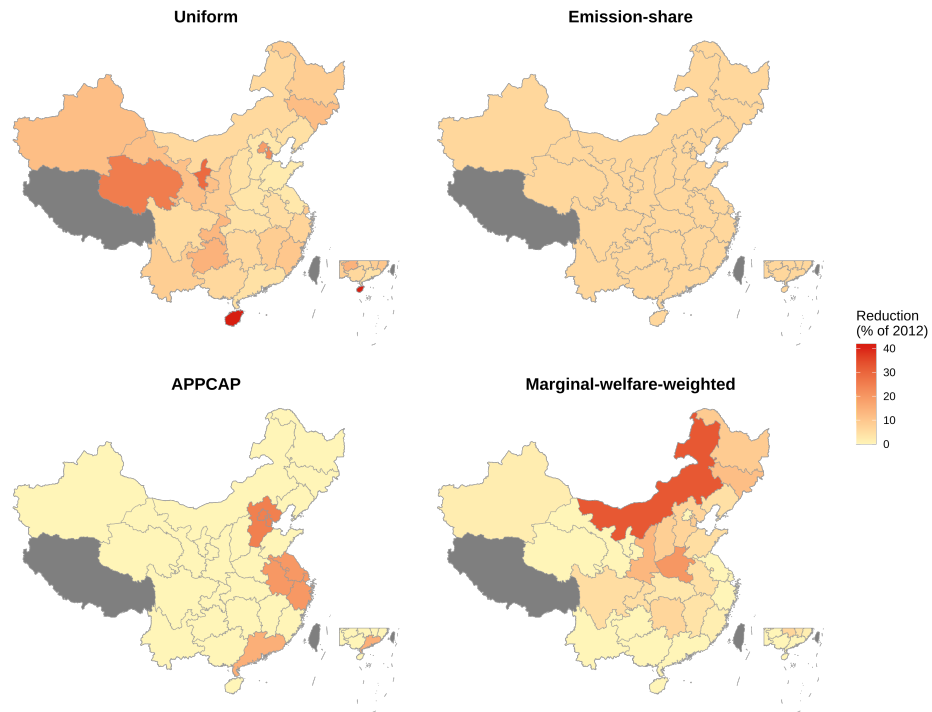
Notes: The Moment column reports the targeted statistic or estimation objective used to calibrate each parameter. The 2002 regional I-O table is used to calibrate the factor shares in the production function, which are held constant across time. Emission elasticity is calibrated targeting emission productivity (see details in Section 5). The emission tax is inverted from the model given λ^j . Trade elasticity, migration elasticity, trade cost, migration cost use values from the literature. Damage coefficients are estimated using 2SLS estimation with thermal inversion as IV. Productivity and amenity are also inverted from the model with observable data on value-added and migration flows. Deposition rate is calibrated so that the model-implied PM_{2.5} concentration is consistent with the data. EDGAR represents PM_{2.5} emission data from Emissions Database for Global Atmospheric Research; CSY represents China Statistical Yearbook; SatPM represents satellite-derived PM_{2.5} concentration data from Washington University in St. Louis.

Appendix Table A7: CEV (%) at $\theta = 0.5$ and $\theta = 1$ by Province

Name	$\theta = 0.5$	$\theta = 1$
Inner Mongolia	1.39	2.38
Henan	0.83	1.54
Shaanxi	0.33	0.76
Liaoning	0.21	0.57
Sichuan	0.37	0.39
Jilin	0.22	0.38
Xinjiang	0.06	0.34
Ningxia	0.00	0.30
Gansu	0.07	0.19
Tianjin	-0.12	0.18
Heilongjiang	0.08	0.13
Qinghai	0.06	0.01
Hainan	-0.17	-0.18
Hunan	-0.20	-0.44
Yunnan	-0.11	-0.47
Guizhou	-0.37	-0.48
Shanghai	-0.06	-0.48
Hebei	-0.33	-0.54
Zhejiang	-0.71	-0.82
Jiangxi	-0.47	-0.82
Aggregate	-0.87	-0.99
Fujian	-0.71	-1.17
Beijing	-0.97	-1.27
Guangdong	-0.84	-1.32
Chongqing	-1.22	-1.77
Hubei	-1.84	-2.18
Guangxi	-1.88	-2.74
Shandong	-2.54	-2.99
Shanxi	-2.80	-2.99
Anhui	-2.43	-3.00
Jiangsu	-3.28	-3.99

Notes: Entries report consumption-equivalent welfare (CEV, %) relative to the $\theta = 0$ benchmark for each province and for the aggregate (listed as "Aggregate").

Appendix Figure A4: Emission Reduction Burden under Different Allocation Rule



Notes: Each panel maps the province-level reduction burden, expressed in percent of 2012 emissions, needed to meet the same national target M under four allocation rules. Panel (a) shows uniform allocation: every province cuts the same amount, so the percent cut is larger where baseline emissions are small. Panel (b) shows Emission-share allocation: cuts are proportional to 2012 emissions, yielding uniform percent reductions. Panel (c) reflects Chinese Air Pollution Prevention and Control Action Plan: JJJ regions, Yangtze River Delta and Pearl River Delta are given 25%, 20% and 15% of total reduction, and rest is shared by remaining provinces based on emission share. Panel (d) shows marginal-welfare-weighted: cuts are proportional to the positive welfare gradient g_n , concentrating effort in upwind source provinces.

2 Solving Algorithm

Given an initial distribution of workers $\{L_0^n\}_{n=1}^N$, initial pollutant concentrations $\{E_0^n\}_{n=1}^N$ and an endowment of structures $H = \{H^{nj}\}_{n=1,j=1}^{N,J}$, initial migration share $\mu_{-1}^{n,i}$, a path of fundamentals $\left\{A_t^{nj}, \bar{B}_t^n, \kappa_t^{ni,ij}, \tau^{n,i}, \psi_t^{nj}\right\}_{n=1,j=1,t=0}^{N,J,\infty}$, parameters $\{\gamma^{nj}, \xi^{nj}, \gamma^{nk,nj}, \lambda^j, \alpha^j\}$, the discount factor (β), trade elasticity $\{\theta^j\}_{j=1}^J$, migration elasticity ν and correlation matrix ρ , we can solve the equilibrium in the following steps:

1. **Guess value changes:** Guess a sequence of $\{Y_{t+1}^n\}_{n=1,t=0}^{N,T}$, with $Y_{T+1}^n = 1$ for all n .
2. **Get migration:** Given $\mu_{-1}^{n,i}$ and $\{Y_{t+1}^n\}_{n=1,t=0}^{N,T}$, use equation (8) to calculate all $\{\mu_{t-1}^{n,i}\}_{t=1}^T$.
3. **Get labour allocation:** Given $\{\mu_{t-1}^{n,i}\}_{t=1}^T$ and $\{L_0^n\}_{n=1}^N$, use equation (9) to calculate all $\{L_t^n\}_{n=1,t=1}^{N,T}$.
4. **Solve for temporary equilibrium:** for $0 \leq t \leq T$
 - (a) **Get amenity and productivity:** Given pollutant concentrations $\{E_t^n\}_{n=1,t=0}^{N,T}$, calculate amenity and production using (13) and (14).
 - (b) **Get wage and labour distribution by region-sector:** Given $\{L_t^n\}_{n=1,t=1}^{N,T}$, use equations (15), (16), and (17) to calculate factor prices $\{w_t^n\}_{n=1}^N$ and $\left\{L_t^{nj}\right\}_{n=1,j=1}^{N,J}$ for each period.
 - (c) **Get emission:** Calculate emissions $\left\{e_t^{nj}\right\}_{n=1,j=1}^{N,J}$ for each period using (18).
 - (d) **Get next period pollutant concentrations:** Given emissions $\left\{e_t^{nj}\right\}_{n=1,j=1}^{N,J}$, calculate next period pollutant concentrations using (??).
5. **Get new value changes:** Using factor prices calculated in step 4 and equation (7) to calculate the new value changes $\{Y_{t+1}^n\}_{n=1,t=0}^{N,T-1}$.
6. **Iteration:** Compare with the initial guess in step 1 and iterate until convergence.

3 Invert Productivity

- Guess A_t^{ij}
- Solve the full static model given L_t^n
 - Guess w_t^n and L_t^{nj} , calculate r_t^{nj}

$$r_t^{nj} = \frac{w_t^n L_t^{nj} (1 - \xi^{nj})}{\xi^{nj} H^{nj}}$$

- Get equilibrium unit cost x_t^{nj} and sectoral price index P_t^{nj}

$$x_t^{nj} = \Xi^{nj} \left(\left((w_t^n)^{\xi^{nj}} (r_t^{nj})^{1-\xi^{nj}} \right)^{\gamma^{nj}} \prod_{k=1}^J \left(P_t^{nk} \right)^{\gamma^{nj,nk}} \right)^{1-\lambda^j} (\psi^{nj})^{\lambda^j}$$

$$P_t^{nj} = \Gamma \left(1 + \frac{1 - \eta^{nj}}{\theta^j} \right)^{1/(1-\eta^{nj})} \left(\sum_{i=1}^N \left(\kappa_t^{nj,ij} x_t^{ij} \right)^{-\theta^j} \left(A_t^{ij} \right)^{\theta^j \gamma^{ij}(1-\lambda^j)} \right)^{-1/\theta^j}$$

- Solve trade share

$$\pi_t^{nj,ij} = \frac{\left(\kappa_t^{nj,ij} x_t^{ij} \right)^{-\theta^j} \left(A_t^{ij} \right)^{\theta^j \gamma^{ij}(1-\lambda^j)}}{\sum_{m=1}^N \left(\kappa_t^{nj,mj} x_t^{mj} \right)^{-\theta^j} \left(A_t^{mj} \right)^{\theta^j \gamma^{mj}(1-\lambda^j)}}$$

- Solve emission

$$e_t^{nj} = \frac{w_t^n L_t^{nj}}{\xi^{nj} \gamma^{nj}} \frac{\lambda^j}{1 - \lambda^j} \frac{1}{\psi^{nj}}$$

- Solve total income

$$I_t^n = w_t^n L_t^n + \sum_k \left(r_t^{nk} H^{nk} + \psi^{nk} e_t^{nk} \right)$$

- Solve expenditure

$$X_t^{nj} = \sum_{k=1}^J (1 - \lambda^k) \gamma^{nk,nj} \sum_{i=1}^N \pi_t^{ik,nk} X_t^{ik} + \alpha^j I_t^n$$

- Update new wage and labour w_t^n and L_{nj}

$$w_t^n = \frac{\sum_j \left(\gamma^{nj} (1 - \lambda^j) \xi_{nj} \sum_i \pi_t^{ij,nj} X_t^{ij} \right)}{L_t^n}$$

$$L_t^{nj} = \frac{\gamma^{nj} (1 - \lambda^j) \xi_{nj}}{w_t^n} \sum_i \pi_t^{ij,nj} X_t^{ij}$$

- Match sectoral value-added

- Value-added of nj has following definition:

$$VA_t^{nj} = \gamma^{nj}(1 - \lambda^j) \sum_i \pi_t^{ij,nj} X_t^{ij}$$

- use data on value-added and trade share equation we can calculate new A_t^{*ij} :

$$(A_t^{*ij})^{-\theta^j \gamma^{ij}(1-\lambda^j)} = \frac{\gamma^{ij}(1-\lambda^j)}{VA_t^{ij}} \sum_n \frac{(\kappa^{nj,ij} x_t^{ij})^{-\theta^j} X_t^{nj}}{\sum_{m=1}^N (\kappa^{nj,mj} x_t^{mj})^{-\theta^j} (A_t^{mj})^{\theta^j \gamma^{mj}(1-\lambda^j)}}$$

The derivation is as follows:

$$\begin{aligned} \pi_t^{nj,ij} &= \frac{(\kappa^{nj,ij} x_t^{ij})^{-\theta^j} (A_t^{ij})^{\theta^j \gamma^{ij}(1-\lambda^j)}}{\sum_{m=1}^N (\kappa^{nj,mj} x_t^{mj})^{-\theta^j} (A_t^{mj})^{\theta^j \gamma^{mj}(1-\lambda^j)}} \\ X_t^{nj} \pi_t^{nj,ij} &= X_t^{nj} \frac{(\kappa^{nj,ij} x_t^{ij})^{-\theta^j} (A_t^{ij})^{\theta^j \gamma^{ij}(1-\lambda^j)}}{\sum_{m=1}^N (\kappa^{nj,mj} x_t^{mj})^{-\theta^j} (A_t^{mj})^{\theta^j \gamma^{mj}(1-\lambda^j)}} \\ \gamma^{ij}(1-\lambda^j) \sum_n X_t^{nj} \pi_t^{nj,ij} &= \gamma^{ij}(1-\lambda^j) \sum_n X_t^{nj} \frac{(\kappa^{nj,ij} x_t^{ij})^{-\theta^j} (A_t^{ij})^{\theta^j \gamma^{ij}(1-\lambda^j)}}{\sum_{m=1}^N (\kappa^{nj,mj} x_t^{mj})^{-\theta^j} (A_t^{mj})^{\theta^j \gamma^{mj}(1-\lambda^j)}} \\ VA_t^{ij} &= (A_t^{ij})^{\theta^j \gamma^{ij}(1-\lambda^j)} \gamma^{ij}(1-\lambda^j) \sum_n \frac{(\kappa^{nj,ij} x_t^{ij})^{-\theta^j} X_t^{nj}}{\sum_{m=1}^N (\kappa^{nj,mj} x_t^{mj})^{-\theta^j} (A_t^{mj})^{\theta^j \gamma^{mj}(1-\lambda^j)}} \\ (A_t^{ij})^{-\theta^j \gamma^{ij}(1-\lambda^j)} &= \frac{\gamma^{ij}(1-\lambda^j)}{VA_t^{ij}} \sum_n \frac{(\kappa^{nj,ij} x_t^{ij})^{-\theta^j} X_t^{nj}}{\sum_{m=1}^N (\kappa^{nj,mj} x_t^{mj})^{-\theta^j} (A_t^{mj})^{\theta^j \gamma^{mj}(1-\lambda^j)}} \end{aligned}$$

- Update A_t^{ij} using A_t^{*ij}

4 Invert Amenity

- Solve for migration cost under the assumption that $\tau^{nj,nj} = 1$ and $\tau^{n,i} = \tau^{i,n}$

$$\frac{\mu_t^{n,i} \mu_t^{i,n}}{\mu_t^{n,n} \mu_t^{i,i}} = \exp(-2\tau^{n,i})^{1/\nu}$$

- Solve for expected utility V_{t+1}^i

$$\begin{aligned}\mu_t^{n,i} &= \frac{\exp(\beta V_{t+1}^i - \tau^{n,i})^{1/\nu}}{\sum_{m=1}^N \exp(\beta V_{t+1}^m - \tau^{n,m})^{1/\nu}} = \frac{(e^{\beta V_{t+1}^i - \tau^{n,i}})^{1/\nu}}{\sum_{m=1}^N (e^{\beta V_{t+1}^m - \tau^{n,m}})^{1/\nu}} \\ \mu_t^{n,i} &= \frac{e^{-\frac{\tau^{n,i}}{\nu}}}{\sum_{m=1}^N (e^{\beta V_{t+1}^m - \tau^{n,m}})^{1/\nu}} \times e^{\frac{\beta V_{t+1}^i}{\nu}} \\ \frac{\mu_t^{n,i}}{e^{-\frac{\tau^{n,i}}{\nu}}} \sum_{m=1}^N e^{-\frac{\tau^{n,m}}{\nu}} e^{\frac{\beta V_{t+1}^m}{\nu}} &= e^{\frac{\beta V_{t+1}^i}{\nu}} \\ \tilde{D} e^{\frac{\beta V_{t+1}^m}{\nu}} &= e^{\frac{\beta V_{t+1}^i}{\nu}}\end{aligned}$$

let $n = i$, then $\sum_{m=1}^N \frac{\mu_t^{i,i}}{e^{-\frac{\tau^{i,i}}{\nu}}} e^{-\frac{\tau^{i,m}}{\nu}} \times e^{\frac{\beta V_{t+1}^m}{\nu}} = e^{\frac{\beta V_{t+1}^i}{\nu}}$, thus we have

$$\tilde{D} \begin{pmatrix} e^{\frac{\beta V_{t+1}^1}{\nu}} \\ \dots \\ e^{\frac{\beta V_{t+1}^{N-1}}{\nu}} \\ e^{\frac{\beta V_{t+1}^N}{\nu}} \end{pmatrix} = \begin{pmatrix} e^{\frac{\beta V_{t+1}^1}{\nu}} \\ \dots \\ e^{\frac{\beta V_{t+1}^{N-1}}{N}} \\ e^{\frac{\beta V_{t+1}^N}{\nu}} \end{pmatrix}$$

Solving the above system of equations gives us $\{V_{t+1}^n\}_{n=1}^N$.

- Solve for amenity

$$\begin{aligned}V_t^n &= \log \frac{B_t^n I_t^n}{P_t^n L_t^n} + \nu \log \left(\sum_{i=1}^N \exp(\beta V_{t+1}^i - \tau^{n,i})^{\frac{1}{\nu}} \right) \\ \log B_t^n &= V_t^n - \log \frac{I_t^n}{P_t^n L_t^n} - \nu \log \left(\sum_{i=1}^N \exp(\beta V_{t+1}^i - \tau^{n,i})^{\frac{1}{\nu}} \right)\end{aligned}$$

5 Calculating Marginal Welfare Effects of Provincial Emission Taxes

This section describes how we calculate the marginal social welfare of emission tax.

Step 1: Define a province-level tax

Let $m \in \{1, \dots, N\}$ index provinces, $j \in \{1, \dots, J\}$ index sectors, and $t^* = 2017$ be the perturbation year. Denote by ψ_{mjt} the tax levied in province m , sector j , at time t , and by E_{mjt} the corresponding emissions.

Define the province-level tax is the emission-weighted average of sectoral taxes:

$$\psi_m \equiv \sum_{j=1}^J s_{mj} \tau_{mj,t^*}, \quad s_{mj} \equiv \frac{E_{mj,t^*}}{\sum_{k=1}^J E_{mk,t^*}}, \quad \sum_{j=1}^J s_{mj} = 1.$$

Intuition: ψ_m is the price a marginal unit of emissions faces in province m in year t^* when the ton is distributed across sectors in proportion to that year's emission mix.

Step 2: Choose the step h in province space

Pick an absolute step in ψ_m , $h = 0.005$, so your central difference spans $2h = 1$ percentage point:

$$\frac{\Delta W}{\Delta \psi_m} \approx \frac{W(\psi_m + h) - W(\psi_m - h)}{2h}$$

Step 3: Map the province step into sectoral moves

We want sectoral changes $\{\Delta \tau_{mj}\}$ such that the emission-weighted average changes by exactly $\pm h$:

$$\sum_j s_{mj} \Delta \tau_{mj} = \pm h.$$

A convenient and transparent choice is to change sectoral rates in proportion to their emission shares, but rescaled so the weighted average is exactly $\pm h$:

$$\Delta \tau_{mj}^{(\pm)} = \pm \frac{hs_{mj}}{\sum_k s_{mk}^2}$$

Then

$$\sum_j s_{mj} \Delta \tau_{mj}^{(\pm)} = \pm h,$$

and sectors that account for more of the province's emissions move more.

Step 4: Implement changes to sectoral emission tax

Implement the shocks at $t = 2017$ and keep them fixed thereafter:

$$\tau_{mj,2017}^{(+)} = \tau_{mj,2017} + \Delta \tau_{mj}^{(+)}, \quad \tau_{mj,2017}^{(-)} = \tau_{mj,2017} + \Delta \tau_{mj}^{(-)}$$

Re-solve the model, and compute welfare W_i and aggregate using $w_i = L_i^{2002} / \sum_k L_k^{2002}$.